A transcriptional regulatory atlas of coronavirus infection of human cells

Scott A Ochsner & Neil J McKenna

The Signaling Pathways Project and Department of Molecular and Cellular Biology, Baylor College of Medicine, Houston, TX 77030

Address Correspondence To:

Neil J. McKenna

Department of Molecular and Cellular Biology

Baylor College of Medicine

Houston, TX 77030

USA

e: nmckenna@bcm.edu

t: 713-798-8568

Abstract

Identifying transcriptional responses that are most consistently associated with experimental coronavirus (CoV) infection can help illuminate human cellular signaling pathways impacted by CoV infection. Here, we distilled over 3,000,000 data points from publically archived CoV infection transcriptomic datasets into consensus regulatory signatures, or consensomes, that rank genes based on their transcriptional responsiveness to infection of human cells by MERS, SARS-CoV-1 and SARS-CoV-2 subtypes. We computed overlap between genes with elevated rankings in the CoV consensomes against those from transcriptomic and ChIP-Seq consensomes for nearly 880 cellular signaling pathway nodes. Validating the CoV infection consensomes, we identified robust overlap between their highly ranked genes and high confidence targets of signaling pathway nodes with known roles in CoV infection. We then developed a series of use cases that illustrate the utility of the CoV consensomes for hypothesis generation around mechanistic aspects of the cellular response to CoV infection. We make the CoV infection datasets and their universe of underlying data points freely accessible through the Signaling Pathways Project web knowledgebase at https://www.signalingpathways.org/datasets/index.jsf.

Introduction

Infection by coronaviruses (CoV) represents a major current global public health concern. Signaling within and between airway epithelial and immune cells in response to infections by CoV and other viruses is coordinated by a complex network of signaling pathway nodes. These include chemokine and cytokine-activated receptors, signaling enzymes and transcription factors, and the genomic targets encoding their downstream effectors (Takeda et al., 2003; Stark et al., 1998; Darnell et al., 1994)]. We recently described the Signaling Pathways Project (SPP; (Ochsner et al., 2019), an integrated 'omics knowledgebase designed to assist bench researchers in leveraging publically archived transcriptomic and ChIP-Seq datasets to generate research hypotheses. A unique aspect of SPP is its collection of consensus regulatory signatures, or consensomes, which rank genes based on the frequency of their significant differential expression across transcriptomic experiments mapped to a specific signaling pathway node or node family. By surveying across multiple independent datasets, we have shown that consensomes recapitulate pathway node-genomic target regulatory relationships to a high confidence level (Ochsner et al., 2019).

Placing the transcriptional events associated with human CoV infection in context with those associated with other signaling paradigms has the potential to catalyze the development of novel therapeutic approaches. The CoV research community has been active in generating and archiving transcriptomic datasets documenting the transcriptional response of human cells to infection by the three major CoV species, namely, Middle East respiratory syndrome coronavirus (MERS) and severe acute respiratory syndrome coronaviruses 1 (SARS1) and 2 (SARS2) (DeDiego et al., 2011;

Josset et al., 2013; Sims et al., 2013; Yoshikawa et al., 2010). To date however the field has lacked a resource that fully capitalizes on these datasets by, firstly, using them to rank human genes according to their transcriptional response to CoV infection and secondly, contextualizing these transcriptional responses by integrating them with 'omics data points relevant to host cellular signaling pathways. Here, as a service to the research community to catalyze the development of novel CoV therapeutics, we generated consensomes for infection of human cells by MERS, SARS1 and SARS2 CoVs. We then analyzed the extent to which high confidence transcriptional targets for these viruses intersected with genes with elevated rankings in transcriptomic and ChIP-Seq consensomes for cellular signaling pathway nodes. Integration of the CoV consensomes with the existing universes of SPP transcriptomic and ChIP-Seq data points in a series of use cases illuminates previously uncharacterized intersections between CoV infection and human cellular signaling pathways. The CoV infection consensome and its underlying datasets provide researchers with a unique and freely accessible framework within which to generate and pressure test hypotheses around human cellular signaling pathways impacted by CoV infection.

Results

Generation of the CoV consensomes

We first set out to generate a set of consensomes ranking human genes based on the frequency of their significant differential expression in response to infection by MERS, SARS1 and SARS2 CoVs. To do this we searched the Gene Expression Omnibus (GEO) and ArrayExpress databases to identify datasets involving infection of human cells by these species. From this initial collection of datasets, we next carried out a three step quality control check as previously described (Ochsner et al., 2019), yielding a total of 3,041,047 million data points in 111 experiments from 25 independent CoV infection transcriptomic datasets (Supplementary information, Section 1). Using these curated datasets, we next generated consensomes for each CoV species, as well as one ranking genes across all CoV infection experiments (ALL CoV). As a reference consensome for a virus whose transcriptional impact on human cells has been studied in depth, we also generated a consensome for human influenza A virus (IAV) infection.

The Supplementary information files contain the full human ALL CoV (Section 2), MERS (Section 3), SARS1 (Section 4), SARS2 (Section 5) and IAV (Section 6) infection transcriptomic consensomes. To assist researchers in inferring transcriptional regulation of signaling networks, the ALL CoV consensome is annotated to indicate the identity of a gene as encoding a bioactive small molecule, receptor, signaling enzyme or transcription factor (Supplementary information, Section 2, columns W-Z). As an initial benchmark for the ALL CoV consensome, we assembled a list of 20 interferon-stimulated genes (ISGs), which encode many of the key canonical viral response factors (Supplementary information, Section 2, column I) (Schneider et al., 2014). As

shown in the scatterplot representation of the ALL COV consensome in Figure 1, all canonical ISGs were assigned appropriately elevated rankings in the consensome.

To gain insight into transcriptional intersections between CoV infection and human cellular signaling pathways, we next computed genes with elevated rankings in the CoV consensomes against genes with high confidence regulatory relationships with cellular signaling pathway nodes. To do this we generated five lists of genes corresponding to the ALL CoV, MERS, SARS1, SARS2 and IAV transcriptomic consensome 95th percentiles. We then retrieved genes in the 95th percentiles of human transcriptomic (n = 30) consensomes and ChIP-Seq (n = 834) consensomes for a collection of cellular signaling pathway nodes, and computed the extent and significance of their overlap with genes in the 95th percentiles of each of the five CoV consensomes. Significant overlap between the 95th percentiles of a node/node family consensome and a CoV consensome would indicate a potential biological relationship between loss or gain of function of that node and the transcriptional response to CoV infection.

For clarity and brevity we will refer from here on to the 95th percentile of a ChIP-Seq consensome as “CC95” and the 95th percentile of a transcriptomic consensome as “TC95”. Of the 834 node CC95s evaluated, 377 had significant overlap ($p < 0.05$) with at least one of the CoV infection TC95s; of the 30 node/node family TC95s evaluated, 25 had significant overlap ($p< 0.05$) with at least one of the CoV infection TC95s. Results of these analyses are shown in Figure 2 (receptor and enzyme transcriptomic analysis), Figure 3 (ChIP-Seq transcription factor analysis), Figure 4 (ChIP-Seq enzyme analysis) and Figure 5 (ChIP-Seq co-node analysis); see also Supplementary information Section 7 for the complete numerical data. We next surveyed the significant overlaps to identify

(i) canonical inflammatory signaling pathway nodes with characterized roles in the response to CoV infection, thereby validating the consensome approach in this context; and (ii) evidence for previously uncharacterized transcriptional biology of CoV infection that are consistent with their roles in the response to other viral infections.

Receptors Reflecting their well-documented roles in the response to viral infection**,** we observed appreciable significant overlap between all TC95s and those for the toll-like (TLR (Totura et al., 2015), interferon (IFNR (Hensley et al., 2004)) and tumor necrosis factor (TNFR (W. Wang et al., 2007)) receptor families (Fig. 2). Interestingly, these signatures were particularly highly enriched in the SARS2 TC95 – potentially reflecting a particularly strong antiviral response to infection by SARS2. TC95 overlaps for receptor systems with previously uncharacterized connections to CoV infection, including epidermal growth factor receptors, glucocorticoid receptor and NOTCH receptor signaling, are consistent with the known roles of these receptor systems in the context of other viral infections (Hayward, 2004; Ito et al., 2011; Ng et al., 2013; Ostler et al., 2019; Zheng et al., 2014). The relatively strong enrichment for xenobiotic receptors reflects work describing a role for pregnane X receptor in innate immunity (S. Wang et al., 2014) and points to a potential role for members of this family in the response to CoV infection.

Transcription factors In general, ChIP-Seq enrichments for transcription factors and other nodes were more specific for individual CoV infection TC95s (compare Fig. 2 with Figs 3, 4 and 5). This is likely due to the fact that ChIP-Seq consensomes are based on direct promoter binding by a specific node antigen, whereas transcriptomic consensomes encompass both direct and indirect targets of specific receptor and

enzyme node families. Not unexpectedly – and speaking again to validation of the consensomes - the strongest and most significant CoV TC95 overlaps were observed for CC95s for known transcription factor mediators of the transcriptional response to CoV infection, including members of the NFκB (Ludwig & Planz, 2008; Poppe et al., 2017; Ruckle et al., 2012), IRF (Chiang & Liu, 2018) and STAT (Blaszczyk et al., 2016; Frieman et al., 2007; Garcia-Sastre et al., 1998) transcription factor families. Consistent with its known role in the regulation of interferon-stimulated genes (Hasan et al., 2013), we also observed appreciable overlap between the CC95 for TFEB and the ALL CoV TC95. Moreover, the strong overlap between the GTF2B/TFIIB CC95 and all viral TC95s reflects previous evidence identifying GTF2B as a target for orthomyxovirus (Haas et al., 2018), herpes simplex virus (Gelev et al., 2014) and hepatitis B virus (Haviv et al., 1998).

Enzymes Compared to the roles of receptors and transcription factors in the response to viral infection, the roles of signaling enzymes are less well illuminated – indeed, in the context of CoV infection, they are entirely unstudied. Through their regulation of cell cycle transitions, cyclin-dependent kinases play important roles in the orchestration of DNA replication and cell division, processes that are critical in the viral life cycle. CDK6, which has been suggested to be a critical G1 phase kinase (Bellail et al., 2014; Grossel & Hinds, 2006), has been shown to be targeted by a number of viral infections, including Kaposi's sarcoma-associated herpesvirus (Kaldis et al., 2001) and HIV-1 (Pauls et al., 2014). Consistent with this common role across distinct viral infections, we observed robust overlap between the CDK95 TC95 (Fig. 2) and the CDK6 CC95 (Fig. 4) and those of all viral TC95s. As with the TLRs, IFNRs and TNFRs, which are known to

signal through CDK6 (Cingoz & Goff, 2018; Handschick et al., 2014; Hennessy et al., 2011), overlap with the CDK6 CC95 was particularly strong in the case of the SARS2 TC95 (Fig. 4). CCNT2 is a member of the highly conserved family cyclin family and, along with CDK9, is a member of the viral-targeted p-TEFB complex (Zaborowska et al., 2016). Reflecting a potential general role in viral infection, appreciable overlap was observed between the CCNT2 CC95 and all viral TC95s (Fig. 4). Finally in the context of enzymes, DNA Topoisomerase (TOP1) has been shown to be required for efficient replication of simian virus 40 (Wobbe et al., 1987) and Ebola (Takahashi et al., 2013) viruses. The prominent overlap between its CC95 and those of SARS2 and IAV (Fig. 4) suggest that it may play a similar role in facilitating the replication of these viruses.

Co-nodes We have coined the term “co-nodes” as a convenient catch-all for cellular factors that are not members of the three principal signaling pathway node categories (receptors, enzymes and transcription factors; Ochsner et al., 2019). The breadth of functions encompassed by members of this category reflects the diverse mechanisms employed both by viruses to infect and propagate in cells, as well as by hosts to mount an efficient immune response. Consistent with its characterized role in the recruitment of p-TEFB by IV-1 Tat protein (Schulze-Gahmen et al., 2013), we observed consistently strong enrichment of the AFF4 CC95 in all viral TC95s (Fig. 5). The targeting of CNOT3 for degradation in response to adenoviral infection (Chalabi Hagkarim et al., 2018) is reflected in the significant overlap between its CC95 and the viral TC95s, particularly in the case of the SARS2 (Fig. 5).

By way of additional independent validation of the CoV and IAV consensomes, Gene Set Enrichment Analysis (Subramanian et al., 2005) reflected significant overlap

between the CoV and IAV TC95s and a variety of viral infection and inflammatory transcription factor target gene sets (Supplementary information Section 8).

Use cases

Having established the reliability of the consensome approach in the context of CoV infection, we next wished to use the CoV consensomes to gather evidence to identify previously uncharacterized mediators of the transcriptional response to infection by CoVs and, of particular current interest, SARS2.

Use case 1: consensome redundancy analysis identifies potential uncharacterized players in the response to CoV infection

We previously showed (Figs. 2 and 3) that the overlap of the CoV TC95 genes was most robust among consensomes for members of the IFNR, TLR and TNF receptor families (Fig. 2), and the NFkB, RELA, IRF and STAT transcription factor families (fig. 5). To investigate this further, we ranked genes in the ALL CoV consensome by their aggregate 80th percentile rankings across these consensomes (Supplementary information, Section 2, column V). Transcriptomic consensomes for IFNRs (Section 9), TLRs (Section 10) and TNFRs (Section 11) are provided in Supplementary information, as are links to the ChIP-Atlas lists used to generate the ChIP-Seq consensomes (Section 12).

This redundancy ranking elevates genes with known critical roles in the response to viral infection that are acutely responsive to a spectrum of inflammatory signaling nodes, such as *NCOA7* (Doyle et al., 2018), *STAT* (Chapgier et al., 2009) and *TAP1* (Gruter et al., 1998). Interestingly, genes such as *PSMB9*, *CSRNP1* and *MRPL24* have ALL CoV discovery rates that are comparable to or exceed those of many of the classic viral response ISGs (Fig. 1), but are either largely or completely uncharacterized in the context of viral infection. This use case the reflects the potential of consensome-driven data mining to illuminate novel and potentially therapeutically relevant transcription pathway effectors in the response to CoV infection.

Use case 2: discrimination between genes frequently differentially expressed in response to CoV, but not IAV, infection

We next wished to gain insight into signaling paradigms that were selectively characteristic of CoV infection but not IAV infection. To do this we generated a set of genes that were frequently differentially expressed in response to CoV infection (ALL CoV TC99), but less frequently expressed in response to IAV infection (50^{th} percentile) (Table 1). Interestingly, this group contained two genes encoding transcription factors with well characterized roles in the regulation of oscillatory gene expression, *PER1* and *PER2* (Yamajuku et al., 2010). This led us to speculate that genomic targets of transcriptional regulators of circadian rhythms might be enriched among high confidence CoV-regulated genes, but not IAV-regulated genes. Consistent with this we observed significant overlap between the CC95s of the master circadian transcription factors ARNTL1/BMAL1 and CLOCK (Gaucher et al., 2018) and the CoV TC95, but not

the IAV TC95 (Fig. 2). These data indicate a hitherto uncharacterized intersection between CoV signaling and the cellular oscillatory apparatus. Another gene of note in this group is *INHBA,* encoding activin A, overexpression of which in murine lung gives rise to a phenotype resembling acute respiratory distress-like syndrome (Apostolou et al., 2012), a condition commonly associated with CoV infection (Totura & Bavari, 2019). Other genes in the group provide evidence for the potential mechanisms of infection and propagation of CoVs. *TJAP1,* for example, encodes a member of a family of proteins involved in regulation of tight junctions, shown to be route of porcine epidemic diarrhea coronavirus entry into epithelial cells (Luo et al., 2017). In addition, *GON7* is a member of the KEOPS complex (Wan et al., 2017), which is involved in threonylcarbamoylation of tRNAs, which represent an important host facet of the retroviral life cycle (Jin & Musier-Forsyth, 2019). Interestingly, another critical gene in this tRNA pathway, *YRDC*, is the 19th ranked gene in the ALL CoV consensome (Supplementary information Section 2).

Use case 3: evidence for antagonism between progesterone receptor and interferon receptor signaling in the airway epithelium

Although a lack of clinical data has so far prevented a definitive evaluation of the connection between pregnancy and susceptibility to SARS2 infection in COVID-19, pregnancy has been previously associated with the incidence of viral infectious diseases, particularly respiratory infections (Sappenfield et al., 2013; Siston et al., 2010). We were interested therefore to see consistent overlap between the progesterone receptor (PGR) TC95 and all the viral TC95s, with the enrichment being

particularly evident in the case of the SARS2 TC95 (Fig. 2). To investigate the specific nature of the crosstalk implied by this overlap in the context of the airway epithelium, we first identified a set of 16 genes that were in both the ALL CoV and PGR TC95s. We then retrieved two SPP experiments involving treatment of A549 airway epithelial cells with the PGR full antagonist RU486 (RU), alone or in combination with the GR agonist dexamethasone (DEX). As shown in Figure 6 , there was nearly unanimous correlation in the direction of regulation of all 16 genes in response to CoV infection and PGR loss of function. These data indicate that antagonism between PGR and IFNR signaling in the airway epithelium may predispose pregnant women to infection by SARS2.

Use case 4: evidence for a role for the telomerase catalytic subunit TERT in the interferon response to viral infection

Although telomerase activation has been well characterized in the context of cell immortalization by human tumor virus infection (Gewin et al., 2004; Klingelhutz et al., 1996; Yang et al., 2004), no connection has previously been made between CoV or IAV infection and telomerase. We were therefore intrigued to observe robust overlap between all viral TC95s and that of the telomerase catalytic subunit TERT. In support of this finding, NFkB signaling has been shown to induce expression (Yin et al., 2000) and nuclear translocation (Akiyama et al., 2003) of TERT, and direct co-regulation by telomerase of NFkB-dependent transcription has been linked to chronic inflammation (Ghosh et al., 2012). Inspecting the ALL CoV consensome underlying data points (data not shown) we found that the *TERT* gene was not transcriptionally induced in response to infection by any of the CoVs, indicating that the overlap between its TC95 and those

of the CoVs might occur in response to an upstream regulatory signal. If functional interactions between TERT and inflammatory nodes did indeed take place in response to CoV infection, we anticipated that this would be reflected in close agreement regarding the direction of differential expression of CoV infection-regulated genes in response to perturbation of TERT on the one hand, and on the other, to stimulation of the classic viral response IFNRs. To test this hypothesis, we took the same set of 20 ISGs referred to previously (Fig. 1) and compared their direction of regulation across all experiments underlying the ALL CoV, TERT and IFNR consensomes. For reference, the TERT consensome (Section 13) and its underlying data points (Section 14) are provided in the Supplementary information. With respect to the IFNR and TERT data points, we observed a nearly universal alignment in the direction of regulation of all genes tested with those in the CoV infection experiments (Fig. 6), with agreement in the direction of regulation across 99% of the underlying probesets. We should note that of the 1859 $p < 0.05$ CoV infection ISG data points, we observed repression, rather than induction, in response to CoV infection in 303 (~15%) , which may be attributable to the impact of differences in cell type, cell cycle stage or virus incubation time across the independent experiments. Our results are consistent with a model in which activation of telomerase is a component of the human innate immune response to viral infection.

Use case 5: SARS2 infection of human cells is specifically associated with an epithelial to mesenchymal transition transcriptional signature

Epithelial to mesenchymal transition (EMT) is the process by which epithelial cells lose their polarity and adhesive properties and acquire the migratory and invasive

302 characteristics of mesenchymal stem cells (Lamouille et al., 2014). EMT is known to
303 contribute to pulmonary fibrosis (Hill et al., 2019) and acute interstitial pneumonia (H. Li
304 et al., 2014), both of which have been reported in connection with SARS2 infection in
305 COVID-19 (Adair & Ledermann, 2020; P. Zhou et al., 2020). Moreover, EMT is widely
306 accepted as a core component of the process by which renal tubular cells transform into
307 mesenchymal cells during the development of fibrosis in kidney disease (Y. Liu, 2006),
308 a signature comorbidity of SARS2 infection (Durvasula et al., 2020). Of the 834 CC95s
309 analyzed, overlap ($p < 0.05$) was specific to the SARS2 CC95 for only five; SNAI2/Slug,
310 SOX2, GATA6, CTBP1 and PRMT1. Strikingly, a literature search indicated that these
311 five nodes were connected by documented roles in in the promotion of EMT (Avasarala
312 et al., 2015; Herreros-Villanueva et al., 2013; Martinelli et al., 2017; Nieto, 2002; Sahu
313 et al., 2017). In addition to these nodes, whose C95 genes were exclusively enriched ($p
314 < 0.05$) in the SARS2 C95 genes, we identified several other EMT-linked nodes whose
315 CC95 genes were preferentially enriched ($p < 0.05$) in the SARS2 TC95 genes (Figs. 3-
316 5), including the homeodomain transcription factor SIX2 (C.-A. Wang et al., 2014),
317 SMAD4 (Siraj et al., 2019), and the co-nodes PYGO2 (Chi et al., 2019), SKI (Tecalco-
318 Cruz et al., 2018), BRD7 (T. Liu et al., 2017) and STAG2 (Nie et al., 2019).

319 To investigate this further, we computed overlap between the individual viral TC99s and
320 a list of 335 genes manually curated from the research literature as signature EMT
321 markers (Supplementary information Section 15; Zhao et al., 2015). Consistent with the
322 node consensome enrichment analysis, we observed significant enrichment of
323 members of this gene set within the SARS2 CC99, but not those of the ALL CoV,
324 SARS1, MERS or IAV consensomes (Supplementary information Section 16). One

possible explanation for this was the fact that the SARS2 consensome was comprised of airway epithelial cell lines, whereas the SARS1 and MERS consensomes included non-epithelial cell biosamples (Supplementary information Section 1). To exclude this possibility therefore, we next calculated airway epithelial cell-specific consensomes for SARS1 and MERS and computed overlap of their TC95s against the 864 pathway node/node family CC95s & TC95s. We found that significant overlap with the CoV TC95s remained specific to SARS2 (data not shown), confirming that significant overlap with the EMT node signature was specific to the SARS2 TC99.

We next applied consensome redundancy analysis (see Use case 1) to isolate a set of SARS2 regulated genes (CPV $P < 0.05$) that were high confidence targets (i.e. in the CC80) for at least two of the EMT nodes (SNAI2, SOX2, GATA6, CTBP1 and PRMT1; Supplementary information, Section 4, column M). A literature survey showed that 13 of these 21 genes had a documented connection to EMT (Supplementary information, Section 5, column N). Figure 9 compares the percentile rankings for these genes across the three CoV infection consensomes and the IAV consensome. Although some EMT genes, such as *CXCL2* and *IRF9*, had elevated rankings across all four consensomes, the collective EMT gene signature had a significantly higher mean percentile value in the SARS2 consensome than in each of the three others (Fig. 9).

Although EMT has been associated with infection by transmissible gastroenteritis virus (Xia et al., 2017), this is to our knowledge the first evidence connecting CoV infection, and specifically SARS2 infection, to EMT. Interestingly, several members of the group of SARS2-induced EMT genes have been associated with signature pulmonary comorbidities of CoV infection, including ADAR (Diaz-Pina et al., 2018), CLDN1

(Vukmirovic et al., 2017) and SOD2 (Gao et al., 2008). Of note in the context of these data is the fact that signaling through two SARS2 cellular receptors, ACE2/AT2 and CD147/basigin, has been linked to EMT in the context of organ fibrosis (Kato et al., 2011; Ruster & Wolf, 2011; C. Wang et al., 2018). Moreover, overlap between of the CoV TC95s and the TERT CC95 was particularly robust in the case of SARS2, a finding of potential relevance to the fact that telomerase has been implicated in EMT (Z. Liu et al., 2013). Collectively, our data indicate that EMT warrants further investigation as a SARS2-specific pathological mechanism.

Development of a CoV infection cell signaling knowledgebase

Having validated the ALL CoV consensome, we next wished to make it freely available to the research community for re-use in the characterization of signaling events associated with CoV infection. Firstly, the viral infection datasets were curated accordingly to our previously described protocol (Ochsner et al., 2019) made available for browsing in the SPP Dataset listing (https://www.signalingpathways.org/datasets/index.jsf). As with other SPP datasets, and per FAIR data best practice, CoV infection datasets were associated with detailed descriptions, assigned a digital object identifier, and linked to the associated article to place the dataset in its original experimental context. Loading the CoV datasets into the SPP also automatically made the underlying data points discoverable by the SPP query tool Ominer (Ochsner et al., 2019). These reports represent a summary of the current state of transcriptomic and ChIP-Seq knowledge on the regulatory relationship of a given gene with upstream regulatory pathway nodes, or in clinical and model experiments. The full value of the integration of the CoV consensome with the existing

SPP framework can perhaps be best appreciated in the context of the one click links to Ominer Regulation Reports from the individual CoV datasets. These Reports provide researchers with a wealth of contextual data on signaling pathways impacted by CoV infection in the context of a specific gene. Table 2 shows links to Regulation Reports for the top twenty ranked genes in the ALL CoV consensome. The order of sections in the Reports is Receptors, Enzymes, Transcription Factors, Co-nodes, Clinical and Models, the last section including data points from the CoV infection model experiments that form the basis of this study.

Discussion

An effective research community response to the impact of CoVs on human health demands systematic exploration of the transcriptional interface between viral infection and human cell signaling systems. It also demands routine access to existing datasets that is unhindered either by paywalls or by lack of the informatics training required to manipulate archived datasets in their unprocessed state. Moreover, the substantial logistical obstacles to BSL3 certification only emphasizes the need for fullest possible access to, and re-usability of, existing CoV infection datasets to focus and refine hypotheses prior to carrying out *in vivo* CoV infection experiments. To this end, we generated a set of CoV infection consensomes that rank human genes by the reproducibility of their significant differential expression in response to infection of human cells by CoVs. We then computed the CoV consensomes against high confidence transcriptional signatures for a broad range of cellular signaling pathway nodes, affording investigators with a broad range of signaling interests an entrez into the study of CoV infection of human cells. The five use cases described here represent illustrative examples of the types of analyses that users are empowered to carry out in the CoV infection knowledgebase.

To democratize access to the CoV consensome and its >3,000,000 underlying data points by the broadest possible audience, we have integrated them into the SPP database to create a cell signaling knowledgebase for CoV infection. Incorporation of the CoV data points into SPP in this manner places them in the context of millions more existing SPP data points documenting transcriptional regulatory relationships between pathway nodes and their genomic targets. In doing so, we afford users a unique

appreciation of the cellular signaling pathway nodes whose gain or loss of function in response to CoV infection gives rise to these transcriptional patterns.

The human CoV and IAV consensomes and their underlying datasets are “living” resources on SPP that will be updated and versioned with appropriate datasets. This will be particularly important in the case of SARS2, as datasets involving infection of human cells with this virus are necessarily currently limited in number. This will allow for hardening of observations that are intriguing, but whose significance is currently unclear, such as the overlap of the CoV TC95s with the TERT TC95, as well as the enrichment of EMT genes among those with elevated rankings in the SARS2 consensome. We welcome feedback and suggestions from the research community for the future development of the SPP CoV infection consensomes.

Methods

Dataset processing and consensome analysis.

Differential expression values were calculated for each gene in each experiment using the limma analysis package from Bioconductor then committed to the consensome analysis pipeline as previously described (Ochsner et al., 2019). Briefly, the consensome algorithm surveys each experiment across all datasets and ranks genes according to the frequency with which they are significantly differentially expressed. For each transcript, we counted the number of experiments where the significance for differential expression was ≤0.05, and then generated the binomial probability, referred to as the consensome p-value (CPV), of observing that many or more nominally significant experiments out of the number of experiments in which the transcript was assayed, given a true probability of 0.05. A more detailed description of the transcriptomic consensome algorithm is available (Ochsner et al., 2019). The consensomes and underlying datasets were loaded into an Oracle 13c database and made available on the SPP user interface as previously described (Ochsner et al., 2019).

Statistical analysis

Gene Overlap analysis was performed using the Bioconductor GeneOverlap analysis package (https://www.rdocumentation.org/packages/GeneOverlap/versions/1.8.0/topics/GeneOverlap) implemented in R. Briefly, given a whole set I of IDs and two sets $A \in I$ and $B \in I$, and $S = A \cap B$, GeneOverlap calculates the significance of obtaining S. The problem is

formulated as a hypergeometric distribution or a contingency table, which is solved by Fisher's exact test. The universe for the overlap was set at a recent estimate of the total number of coding genes in the human genome (21,500; Pertea et al., 2018). Paired Two Sample t-Test for comparing the mean percentile ranking of EMT genes in the MERS, SARS1, SARS2 and IAV consensomes was performed in PRISM at 12 degrees of freedom.

Consensome generation

The procedure for generating transcriptomic consensomes has been previously described (Ochsner et al., 2019). To generate the ChIP-Seq consensomes, we first retrieved processed gene lists from ChIP-Atlas, which rank human genes based upon their average MACS2 occupancy across all publically archived datasets in which a given transcription factor, enzyme or co-node is the IP antigen. Of the three stringency levels available (10, 5 and 1 kb from the transcription start site), we selected the most stringent (1 kb). According to SPP convention (Ochsner et al., 2019), we then mapped the IP antigen to its pathway node category and class, and the experimental cell line to its appropriate biosample physiological system and organ. We then organized the ranked lists into percentiles to generate the node ChIP-Seq consensome.

SPP web application

The SPP knowledgebase is a gene-centric Java Enterprise Edition 6, web-based application around which other gene, mRNA, protein and BSM data from external databases such as NCBI are collected. After undergoing semiautomated processing and biocuration as described above, the data and annotations are stored in SPP's

Oracle 13c database. RESTful web services exposing SPP data, which are served to responsively designed views in the user interface, were created using a Flat UI Toolkit with a combination of JavaScript, D3.JS, AJAX, HTML5, and CSS3. JavaServer Faces and PrimeFaces are the primary technologies behind the user interface. SPP has been optimized for Firefox 24+, Chrome 30+, Safari 5.1.9+, and Internet Explorer 9+, with validations performed in BrowserStack and load testing in LoadUIWeb. XML describing each dataset and experiment is generated and submitted to CrossRef to mint DOIs (Ochsner et al., 2019).

Data availability

The entire set of data points used to generate the CoV consensome has been uploaded in an R file to Figshare and a link included for reviewer access. The entire set of metadata for these data points is available in Supplementary information Section 1. Consensome data points are in Supplementary information Sections 2-6.

SPP is freely accessible at https://www.signalingpathways.org. Programmatic access to all underlying data points and their associated metadata are supported by a RESTful API at https://www.signalingpathways.org/docs/. All SPP datasets are biocurated versions of publically archived datasets, are formatted according to the recommendations of the FORCE11 Joint Declaration on Data Citation Principles [74], and are made available under a Creative Commons CC 3.0 BY license. The original datasets are available are linked to from the corresponding SPP datasets using the original repository accession identifiers. These identifiers are for transcriptomic datasets, the Gene Expression Omnibus (GEO) Series (GSE); and for cistromic/ChIP-Seq datasets, the NCBI Sequence Read Archive (SRA) study identifier (SRP). DOIs for the consensomes and datasets are pending.

Code availability

The full SPP source code is available in the SPP GitHub account under a Creative Commons CC 3.0 BY license at https://github.com/signaling-pathways-project/ominer/.

Acknowledgements

This work was supported by the National Institute of Diabetes, Digestive and Kidney Diseases NIDDK Information Network U24 (DK097748), the National Cancer Institute (CA125123) and by the Brockman Medical Research Foundation. We appreciate the technical assistance of Apollo McOwiti and Shijing Qu of the Biostatistics and Informatics Shared Resource of the Duncan NCI Comprehensive Cancer Center. We thank all investigators who archive their datasets, without whom SPP would not be possible.

Author contributions

Dataset biocuration: SO

Data analysis: SO, NM

Manuscript drafting: NM

Competing interests

The authors declare no competing interests.

References

Adair, L. B. 2nd, & Ledermann, E. J. (2020). Chest CT Findings of Early and Progressive Phase COVID-19 Infection from a US Patient. In *Radiology case reports*. https://doi.org/10.1016/j.radcr.2020.04.031

Akiyama, M., Hideshima, T., Hayashi, T., Tai, Y.-T., Mitsiades, C. S., Mitsiades, N., Chauhan, D., Richardson, P., Munshi, N. C., & Anderson, K. C. (2003). Nuclear factor-kappaB p65 mediates tumor necrosis factor alpha-induced nuclear translocation of telomerase reverse transcriptase protein. *Cancer Research*, *63*(1), 18–21.

Apostolou, E., Stavropoulos, A., Sountoulidis, A., Xirakia, C., Giaglis, S., Protopapadakis, E., Ritis, K., Mentzelopoulos, S., Pasternack, A., Foster, M., Ritvos, O., Tzelepis, G. E., Andreakos, E., & Sideras, P. (2012). Activin-A overexpression in the murine lung causes pathology that simulates acute respiratory distress syndrome. *American Journal of Respiratory and Critical Care Medicine*, *185*(4), 382–391. https://doi.org/10.1164/rccm.201105-0784OC

Avasarala, S., Van Scoyk, M., Karuppusamy Rathinam, M. K., Zerayesus, S., Zhao, X., Zhang, W., Pergande, M. R., Borgia, J. A., DeGregori, J., Port, J. D., Winn, R. A., & Bikkavilli, R. K. (2015). PRMT1 Is a Novel Regulator of Epithelial-Mesenchymal-Transition in Non-small Cell Lung Cancer. *The Journal of Biological Chemistry*, *290*(21), 13479–13489. https://doi.org/10.1074/jbc.M114.636050

Barata, J. T., Durum, S. K., & Seddon, B. (2019). Flip the coin: IL-7 and IL-7R in health and disease. *Nature Immunology*, *20*(12), 1584–1593. https://doi.org/10.1038/s41590-019-0479-x

Bellail, A. C., Olson, J. J., & Hao, C. (2014). SUMO1 modification stabilizes CDK6 protein and drives the cell cycle and glioblastoma progression. *Nature Communications*, *5*, 4234. https://doi.org/10.1038/ncomms5234

Blaszczyk, K., Nowicka, H., Kostyrko, K., Antonczyk, A., Wesoly, J., & Bluyssen, H. A. R. (2016). The unique role of STAT2 in constitutive and IFN-induced transcription and antiviral responses. *Cytokine & Growth Factor Reviews*, *29*, 71–81. https://doi.org/10.1016/j.cytogfr.2016.02.010

Chalabi Hagkarim, N., Ryan, E. L., Byrd, P. J., Hollingworth, R., Shimwell, N. J., Agathanggelou, A., Vavasseur, M., Kolbe, V., Speiseder, T., Dobner, T., Stewart, G. S., & Grand, R. J. (2018). Degradation of a Novel DNA Damage Response Protein, Tankyrase 1 Binding Protein 1, following Adenovirus Infection. *Journal of Virology*, *92*(12). https://doi.org/10.1128/JVI.02034-17

Chang, B., Yang, H., Jiao, Y., Wang, K., Liu, Z., Wu, P., Li, S., & Wang, A. (2016). SOD2 deregulation enhances migration, invasion and has poor prognosis in salivary adenoid cystic carcinoma. *Scientific Reports*, *6*, 25918. https://doi.org/10.1038/srep25918

546 Chapgier, A., Kong, X.-F., Boisson-Dupuis, S., Jouanguy, E., Averbuch, D., Feinberg,
547 J., Zhang, S.-Y., Bustamante, J., Vogt, G., Lejeune, J., Mayola, E., de
548 Beaucoudrey, L., Abel, L., Engelhard, D., & Casanova, J.-L. (2009). A partial form
549 of recessive STAT1 deficiency in humans. *The Journal of Clinical Investigation*,
550 *119*(6), 1502–1514. https://doi.org/10.1172/JCI37083

551 Chi, Y., Wang, F., Zhang, T., Xu, H., Zhang, Y., Shan, Z., Wu, S., Fan, Q., & Sun, Y.
552 (2019). miR-516a-3p inhibits breast cancer cell growth and EMT by blocking the
553 Pygo2/Wnt signalling pathway. *Journal of Cellular and Molecular Medicine*, *23*(9),
554 6295–6307. https://doi.org/10.1111/jcmm.14515

555 Chiang, H.-S., & Liu, H. M. (2018). The Molecular Basis of Viral Inhibition of IRF- and
556 STAT-Dependent Immune Responses. *Frontiers in Immunology*, *9*, 3086.
557 https://doi.org/10.3389/fimmu.2018.03086

558 Cingoz, O., & Goff, S. P. (2018). Cyclin-dependent kinase activity is required for type I
559 interferon production. *Proceedings of the National Academy of Sciences of the*
560 *United States of America*, *115*(13), E2950–E2959.
561 https://doi.org/10.1073/pnas.1720431115

562 Darnell, J. E. J., Kerr, I. M., & Stark, G. R. (1994). Jak-STAT pathways and
563 transcriptional activation in response to IFNs and other extracellular signaling
564 proteins. *Science (New York, N.Y.)*, *264*(5164), 1415–1421.
565 https://doi.org/10.1126/science.8197455

566 DeDiego, M. L., Nieto-Torres, J. L., Jimenez-Guardeno, J. M., Regla-Nava, J. A.,
567 Alvarez, E., Oliveros, J. C., Zhao, J., Fett, C., Perlman, S., & Enjuanes, L. (2011).
568 Severe acute respiratory syndrome coronavirus envelope protein regulates cell
569 stress response and apoptosis. *PLoS Pathogens*, *7*(10), e1002315.
570 https://doi.org/10.1371/journal.ppat.1002315

571 Diaz-Pina, G., Ordonez-Razo, R. M., Montes, E., Paramo, I., Becerril, C., Salgado, A.,
572 Santibanez-Salgado, J. A., Maldonado, M., & Ruiz, V. (2018). The Role of ADAR1
573 and ADAR2 in the Regulation of miRNA-21 in Idiopathic Pulmonary Fibrosis. *Lung*,
574 *196*(4), 393–400. https://doi.org/10.1007/s00408-018-0115-9

575 Doherty, M. R., Cheon, H., Junk, D. J., Vinayak, S., Varadan, V., Telli, M. L., Ford, J.
576 M., Stark, G. R., & Jackson, M. W. (2017). Interferon-beta represses cancer stem
577 cell properties in triple-negative breast cancer. *Proceedings of the National*
578 *Academy of Sciences of the United States of America*, *114*(52), 13792–13797.
579 https://doi.org/10.1073/pnas.1713728114

580 Doyle, T., Moncorge, O., Bonaventure, B., Pollpeter, D., Lussignol, M., Tauziet, M.,
581 Apolonia, L., Catanese, M.-T., Goujon, C., & Malim, M. H. (2018). The interferon-
582 inducible isoform of NCOA7 inhibits endosome-mediated viral entry. *Nature*
583 *Microbiology*, *3*(12), 1369–1376. https://doi.org/10.1038/s41564-018-0273-9

584 Durvasula, R., Wellington, T., McNamara, E., & Watnick, S. (2020). COVID-19 and
585 Kidney Failure in the Acute Care Setting: Our Experience From Seattle. In

American journal of kidney diseases : the official journal of the National Kidney Foundation. https://doi.org/10.1053/j.ajkd.2020.04.001

Ercolano, G., De Cicco, P., Rubino, V., Terrazzano, G., Ruggiero, G., Carriero, R., Kunderfranco, P., & Ianaro, A. (2019). Knockdown of PTGS2 by CRISPR/CAS9 System Designates a New Potential Gene Target for Melanoma Treatment. *Frontiers in Pharmacology*, *10*, 1456. https://doi.org/10.3389/fphar.2019.01456

Frieman, M., Yount, B., Heise, M., Kopecky-Bromberg, S. A., Palese, P., & Baric, R. S. (2007). Severe acute respiratory syndrome coronavirus ORF6 antagonizes STAT1 function by sequestering nuclear import factors on the rough endoplasmic reticulum/Golgi membrane. *Journal of Virology*, *81*(18), 9812–9824. https://doi.org/10.1128/JVI.01012-07

Gao, F., Kinnula, V. L., Myllarniemi, M., & Oury, T. D. (2008). Extracellular superoxide dismutase in pulmonary fibrosis. *Antioxidants & Redox Signaling*, *10*(2), 343–354. https://doi.org/10.1089/ars.2007.1908

Garcia-Sastre, A., Durbin, R. K., Zheng, H., Palese, P., Gertner, R., Levy, D. E., & Durbin, J. E. (1998). The role of interferon in influenza virus tissue tropism. *Journal of Virology*, *72*(11), 8550–8558.

Gaucher, J., Montellier, E., & Sassone-Corsi, P. (2018). Molecular Cogs: Interplay between Circadian Clock and Cell Cycle. *Trends in Cell Biology*, *28*(5), 368–379. https://doi.org/10.1016/j.tcb.2018.01.006

Gelev, V., Zabolotny, J. M., Lange, M., Hiromura, M., Yoo, S. W., Orlando, J. S., Kushnir, A., Horikoshi, N., Paquet, E., Bachvarov, D., Schaffer, P. A., & Usheva, A. (2014). A new paradigm for transcription factor TFIIB functionality. *Scientific Reports*, *4*, 3664. https://doi.org/10.1038/srep03664

Gewin, L., Myers, H., Kiyono, T., & Galloway, D. A. (2004). Identification of a novel telomerase repressor that interacts with the human papillomavirus type-16 E6/E6-AP complex. *Genes & Development*, *18*(18), 2269–2282. https://doi.org/10.1101/gad.1214704

Ghosh, A., Saginc, G., Leow, S. C., Khattar, E., Shin, E. M., Yan, T. D., Wong, M., Zhang, Z., Li, G., Sung, W.-K., Zhou, J., Chng, W. J., Li, S., Liu, E., & Tergaonkar, V. (2012). Telomerase directly regulates NF-kappaB-dependent transcription. *Nature Cell Biology*, *14*(12), 1270–1281. https://doi.org/10.1038/ncb2621

Grossel, M. J., & Hinds, P. W. (2006). Beyond the cell cycle: a new role for Cdk6 in differentiation. *Journal of Cellular Biochemistry*, *97*(3), 485–493. https://doi.org/10.1002/jcb.20712

Gruter, P., Tabernero, C., von Kobbe, C., Schmitt, C., Saavedra, C., Bachi, A., Wilm, M., Felber, B. K., & Izaurralde, E. (1998). TAP, the human homolog of Mex67p, mediates CTE-dependent RNA export from the nucleus. *Molecular Cell*, *1*(5), 649–659. https://doi.org/10.1016/s1097-2765(00)80065-9

Haas, D. A., Meiler, A., Geiger, K., Vogt, C., Preuss, E., Kochs, G., & Pichlmair, A. (2018). Viral targeting of TFIIB impairs de novo polymerase II recruitment and affects antiviral immunity. *PLoS Pathogens*, *14*(4), e1006980. https://doi.org/10.1371/journal.ppat.1006980

Handschick, K., Beuerlein, K., Jurida, L., Bartkuhn, M., Muller, H., Soelch, J., Weber, A., Dittrich-Breiholz, O., Schneider, H., Scharfe, M., Jarek, M., Stellzig, J., Schmitz, M. L., & Kracht, M. (2014). Cyclin-dependent kinase 6 is a chromatin-bound cofactor for NF-kappaB-dependent gene expression. *Molecular Cell*, *53*(2), 193–208. https://doi.org/10.1016/j.molcel.2013.12.002

Hasan, M., Koch, J., Rakheja, D., Pattnaik, A. K., Brugarolas, J., Dozmorov, I., Levine, B., Wakeland, E. K., Lee-Kirsch, M. A., & Yan, N. (2013). Trex1 regulates lysosomal biogenesis and interferon-independent activation of antiviral genes. *Nature Immunology*, *14*(1), 61–71. https://doi.org/10.1038/ni.2475

Haviv, I., Shamay, M., Doitsh, G., & Shaul, Y. (1998). Hepatitis B virus pX targets TFIIB in transcription coactivation. *Molecular and Cellular Biology*, *18*(3), 1562–1569. https://doi.org/10.1128/mcb.18.3.1562

Hayward, S. D. (2004). Viral interactions with the Notch pathway. *Seminars in Cancer Biology*, *14*(5), 387–396. https://doi.org/10.1016/j.semcancer.2004.04.018

Hennessy, E. J., Sheedy, F. J., Santamaria, D., Barbacid, M., & O'Neill, L. A. J. (2011). Toll-like receptor-4 (TLR4) down-regulates microRNA-107, increasing macrophage adhesion via cyclin-dependent kinase 6. *The Journal of Biological Chemistry*, *286*(29), 25531–25539. https://doi.org/10.1074/jbc.M111.256206

Hensley, L. E., Fritz, L. E., Jahrling, P. B., Karp, C. L., Huggins, J. W., & Geisbert, T. W. (2004). Interferon-beta 1a and SARS coronavirus replication. *Emerging Infectious Diseases*, *10*(2), 317–319. https://doi.org/10.3201/eid1002.030482

Herreros-Villanueva, M., Zhang, J.-S., Koenig, A., Abel, E. V, Smyrk, T. C., Bamlet, W. R., de Narvajas, A. A.-M., Gomez, T. S., Simeone, D. M., Bujanda, L., & Billadeau, D. D. (2013). SOX2 promotes dedifferentiation and imparts stem cell-like features to pancreatic cancer cells. *Oncogenesis*, *2*, e61. https://doi.org/10.1038/oncsis.2013.23

Hill, C., Jones, M. G., Davies, D. E., & Wang, Y. (2019). Epithelial-mesenchymal transition contributes to pulmonary fibrosis via aberrant epithelial/fibroblastic cross-talk. *Journal of Lung Health and Diseases*, *3*(2), 31–35.

Ito, T., Allen, R. M., Carson, W. F. 4th, Schaller, M., Cavassani, K. A., Hogaboam, C. M., Lukacs, N. W., Matsukawa, A., & Kunkel, S. L. (2011). The critical role of Notch ligand Delta-like 1 in the pathogenesis of influenza A virus (H1N1) infection. *PLoS Pathogens*, *7*(11), e1002341. https://doi.org/10.1371/journal.ppat.1002341

Jiang, R., Li, Y., Xu, Y., Zhou, Y., Pang, Y., Shen, L., Zhao, Y., Zhang, J., Zhou, J., Wang, X., & Liu, Q. (2013). EMT and CSC-like properties mediated by the

IKKbeta/IkappaBalpha/RelA signal pathway via the transcriptional regulator, Snail, are involved in the arsenite-induced neoplastic transformation of human keratinocytes. *Archives of Toxicology*, *87*(6), 991–1000. https://doi.org/10.1007/s00204-012-0933-0

Jin, D., & Musier-Forsyth, K. (2019). Role of host tRNAs and aminoacyl-tRNA synthetases in retroviral replication. *The Journal of Biological Chemistry*, *294*(14), 5352–5364. https://doi.org/10.1074/jbc.REV118.002957

Jordan, N. V., Prat, A., Abell, A. N., Zawistowski, J. S., Sciaky, N., Karginova, O. A., Zhou, B., Golitz, B. T., Perou, C. M., & Johnson, G. L. (2013). SWI/SNF chromatin-remodeling factor Smarcd3/Baf60c controls epithelial-mesenchymal transition by inducing Wnt5a signaling. *Molecular and Cellular Biology*, *33*(15), 3011–3025. https://doi.org/10.1128/MCB.01443-12

Josset, L., Menachery, V. D., Gralinski, L. E., Agnihothram, S., Sova, P., Carter, V. S., Yount, B. L., Graham, R. L., Baric, R. S., & Katze, M. G. (2013). Cell host response to infection with novel human coronavirus EMC predicts potential antivirals and important differences with SARS coronavirus. *MBio*, *4*(3), e00165-13. https://doi.org/10.1128/mBio.00165-13

Kaldis, P., Ojala, P. M., Tong, L., Makela, T. P., & Solomon, M. J. (2001). CAK-independent activation of CDK6 by a viral cyclin. *Molecular Biology of the Cell*, *12*(12), 3987–3999. https://doi.org/10.1091/mbc.12.12.3987

Kato, N., Kosugi, T., Sato, W., Ishimoto, T., Kojima, H., Sato, Y., Sakamoto, K., Maruyama, S., Yuzawa, Y., Matsuo, S., & Kadomatsu, K. (2011). Basigin/CD147 promotes renal fibrosis after unilateral ureteral obstruction. *The American Journal of Pathology*, *178*(2), 572–579. https://doi.org/10.1016/j.ajpath.2010.10.009

Klingelhutz, A. J., Foster, S. A., & McDougall, J. K. (1996). Telomerase activation by the E6 gene product of human papillomavirus type 16. *Nature*, *380*(6569), 79–82. https://doi.org/10.1038/380079a0

Kolosionek, E., Savai, R., Ghofrani, H. A., Weissmann, N., Guenther, A., Grimminger, F., Seeger, W., Banat, G. A., Schermuly, R. T., & Pullamsetti, S. S. (2009). Expression and activity of phosphodiesterase isoforms during epithelial mesenchymal transition: the role of phosphodiesterase 4. *Molecular Biology of the Cell*, *20*(22), 4751–4765. https://doi.org/10.1091/mbc.e09-01-0019

Kuo, W.-Y., Wu, C.-Y., Hwu, L., Lee, J.-S., Tsai, C.-H., Lin, K.-P., Wang, H.-E., Chou, T.-Y., Tsai, C.-M., Gelovani, J., & Liu, R.-S. (2015). Enhancement of tumor initiation and expression of KCNMA1, MORF4L2 and ASPM genes in the adenocarcinoma of lung xenograft after vorinostat treatment. *Oncotarget*, *6*(11), 8663–8675. https://doi.org/10.18632/oncotarget.3536

Lamouille, S., Xu, J., & Derynck, R. (2014). Molecular mechanisms of epithelial-mesenchymal transition. *Nature Reviews. Molecular Cell Biology*, *15*(3), 178–196. https://doi.org/10.1038/nrm3758

Li, H., Zhang, J., Song, X., Wang, T., Li, Z., Hao, D., Wang, X., Zheng, Q., Mao, C., Xu, P., & Lv, C. (2014). Alveolar epithelial cells undergo epithelial-mesenchymal transition in acute interstitial pneumonia: a case report. *BMC Pulmonary Medicine*, *14*, 67. https://doi.org/10.1186/1471-2466-14-67

Li, N., Gou, J.-H., Xiong, J., You, J.-J., & Li, Z.-Y. (2020). HOXB4 promotes the malignant progression of ovarian cancer via DHDDS. *BMC Cancer*, *20*(1), 222. https://doi.org/10.1186/s12885-020-06725-4

Liu, T., Zhao, M., Liu, J., He, Z., Zhang, Y., You, H., Huang, J., Lin, X., & Feng, X.-H. (2017). Tumor suppressor bromodomain-containing protein 7 cooperates with Smads to promote transforming growth factor-beta responses. *Oncogene*, *36*(3), 362–372. https://doi.org/10.1038/onc.2016.204

Liu, X., Fu, Y., Huang, J., Wu, M., Zhang, Z., Xu, R., Zhang, P., Zhao, S., Liu, L., & Jiang, H. (2019). ADAR1 promotes the epithelial-to-mesenchymal transition and stem-like cell phenotype of oral cancer by facilitating oncogenic microRNA maturation. *Journal of Experimental & Clinical Cancer Research : CR*, *38*(1), 315. https://doi.org/10.1186/s13046-019-1300-2

Liu, Y. (2006). Renal fibrosis: new insights into the pathogenesis and therapeutics. *Kidney International*, *69*(2), 213–217. https://doi.org/10.1038/sj.ki.5000054

Liu, Z., Li, Q., Li, K., Chen, L., Li, W., Hou, M., Liu, T., Yang, J., Lindvall, C., Bjorkholm, M., Jia, J., & Xu, D. (2013). Telomerase reverse transcriptase promotes epithelial-mesenchymal transition and stem cell-like traits in cancer cells. *Oncogene*, *32*(36), 4203–4213. https://doi.org/10.1038/onc.2012.441

Ludwig, S., & Planz, O. (2008). Influenza viruses and the NF-kappaB signaling pathway - towards a novel concept of antiviral therapy. *Biological Chemistry*, *389*(10), 1307–1312. https://doi.org/10.1515/BC.2008.148

Luo, X., Guo, L., Zhang, J., Xu, Y., Gu, W., Feng, L., & Wang, Y. (2017). Tight Junction Protein Occludin Is a Porcine Epidemic Diarrhea Virus Entry Factor. *Journal of Virology*, *91*(10). https://doi.org/10.1128/JVI.00202-17

Martinelli, P., Carrillo-de Santa Pau, E., Cox, T., Sainz, B. J., Dusetti, N., Greenhalf, W., Rinaldi, L., Costello, E., Ghaneh, P., Malats, N., Buchler, M., Pajic, M., Biankin, A. V, Iovanna, J., Neoptolemos, J., & Real, F. X. (2017). GATA6 regulates EMT and tumour dissemination, and is a marker of response to adjuvant chemotherapy in pancreatic cancer. *Gut*, *66*(9), 1665–1676. https://doi.org/10.1136/gutjnl-2015-311256

Mendoza-Rodriguez, M., Arevalo Romero, H., Fuentes-Panana, E. M., Ayala-Sumuano, J.-T., & Meza, I. (2017). IL-1beta induces up-regulation of BIRC3, a gene involved in chemoresistance to doxorubicin in breast cancer cells. *Cancer Letters*, *390*, 39–44. https://doi.org/10.1016/j.canlet.2017.01.005

Ng, S. S. M., Li, A., Pavlakis, G. N., Ozato, K., & Kino, T. (2013). Viral infection

743 increases glucocorticoid-induced interleukin-10 production through ERK-mediated
744 phosphorylation of the glucocorticoid receptor in dendritic cells: potential clinical
745 implications. *PloS One*, *8*(5), e63587. https://doi.org/10.1371/journal.pone.0063587

746 Nie, Z., Gao, W., Zhang, Y., Hou, Y., Liu, J., Li, Z., Xue, W., Ye, X., & Jin, A. (2019).
747 STAG2 loss-of-function mutation induces PD-L1 expression in U2OS cells. *Annals*
748 *of Translational Medicine*, *7*(7), 127. https://doi.org/10.21037/atm.2019.02.23

749 Nieto, M. A. (2002). The snail superfamily of zinc-finger transcription factors. *Nature*
750 *Reviews. Molecular Cell Biology*, *3*(3), 155–166. https://doi.org/10.1038/nrm757

751 Ochsner, S. A., Abraham, D., Martin, K., Ding, W., McOwiti, A., Kankanamge, W.,
752 Wang, Z., Andreano, K., Hamilton, R. A., Chen, Y., Hamilton, A., Gantner, M. L.,
753 Dehart, M., Qu, S., Hilsenbeck, S. G., Becnel, L. B., Bridges, D., Ma'ayan, A.,
754 Huss, J. M., … McKenna, N. J. (2019). The Signaling Pathways Project, an
755 integrated 'omics knowledgebase for mammalian cellular signaling pathways.
756 *Scientific Data*, *6*(1), 252. https://doi.org/10.1038/s41597-019-0193-4

757 Ostler, J. B., Harrison, K. S., Schroeder, K., Thunuguntla, P., & Jones, C. (2019). The
758 Glucocorticoid Receptor (GR) Stimulates Herpes Simplex Virus 1 Productive
759 Infection, in Part Because the Infected Cell Protein 0 (ICP0) Promoter Is
760 Cooperatively Transactivated by the GR and Kruppel-Like Transcription Factor 15.
761 *Journal of Virology*, *93*(6). https://doi.org/10.1128/JVI.02063-18

762 Pauls, E., Ruiz, A., Badia, R., Permanyer, M., Gubern, A., Riveira-Munoz, E., Torres-
763 Torronteras, J., Alvarez, M., Mothe, B., Brander, C., Crespo, M., Menendez-Arias,
764 L., Clotet, B., Keppler, O. T., Marti, R., Posas, F., Ballana, E., & Este, J. A. (2014).
765 Cell cycle control and HIV-1 susceptibility are linked by CDK6-dependent CDK2
766 phosphorylation of SAMHD1 in myeloid and lymphoid cells. *Journal of Immunology*
767 *(Baltimore, Md. : 1950)*, *193*(4), 1988–1997.
768 https://doi.org/10.4049/jimmunol.1400873

769 Pertea, M., Shumate, A., Pertea, G., Varabyou, A., Breitwieser, F. P., Chang, Y.-C.,
770 Madugundu, A. K., Pandey, A., & Salzberg, S. L. (2018). CHESS: a new human
771 gene catalog curated from thousands of large-scale RNA sequencing experiments
772 reveals extensive transcriptional noise. *Genome Biology*, *19*(1), 208.
773 https://doi.org/10.1186/s13059-018-1590-2

774 Poppe, M., Wittig, S., Jurida, L., Bartkuhn, M., Wilhelm, J., Muller, H., Beuerlein, K.,
775 Karl, N., Bhuju, S., Ziebuhr, J., Schmitz, M. L., & Kracht, M. (2017). The NF-
776 kappaB-dependent and -independent transcriptome and chromatin landscapes of
777 human coronavirus 229E-infected cells. *PLoS Pathogens*, *13*(3), e1006286.
778 https://doi.org/10.1371/journal.ppat.1006286

779 Ruckle, A., Haasbach, E., Julkunen, I., Planz, O., Ehrhardt, C., & Ludwig, S. (2012).
780 The NS1 protein of influenza A virus blocks RIG-I-mediated activation of the
781 noncanonical NF-kappaB pathway and p52/RelB-dependent gene expression in
782 lung epithelial cells. *Journal of Virology*, *86*(18), 10211–10217.
783 https://doi.org/10.1128/JVI.00323-12

784 Ruster, C., & Wolf, G. (2011). Angiotensin II as a morphogenic cytokine stimulating
785 renal fibrogenesis. *Journal of the American Society of Nephrology : JASN*, *22*(7),
786 1189–1199. https://doi.org/10.1681/ASN.2010040384

787 Sahu, S. K., Tiwari, N., Pataskar, A., Zhuang, Y., Borisova, M., Diken, M., Strand, S.,
788 Beli, P., & Tiwari, V. K. (2017). FBXO32 promotes microenvironment underlying
789 epithelial-mesenchymal transition via CtBP1 during tumour metastasis and brain
790 development. *Nature Communications*, *8*(1), 1523. https://doi.org/10.1038/s41467-
791 017-01366-x

792 Sappenfield, E., Jamieson, D. J., & Kourtis, A. P. (2013). Pregnancy and susceptibility
793 to infectious diseases. *Infectious Diseases in Obstetrics and Gynecology*, *2013*,
794 752852. https://doi.org/10.1155/2013/752852

795 Schneider, W. M., Chevillotte, M. D., & Rice, C. M. (2014). Interferon-stimulated genes:
796 a complex web of host defenses. *Annual Review of Immunology*, *32*, 513–545.
797 https://doi.org/10.1146/annurev-immunol-032713-120231

798 Schulze-Gahmen, U., Upton, H., Birnberg, A., Bao, K., Chou, S., Krogan, N. J., Zhou,
799 Q., & Alber, T. (2013). The AFF4 scaffold binds human P-TEFb adjacent to HIV
800 Tat. *ELife*, *2*, e00327. https://doi.org/10.7554/eLife.00327

801 Sims, A. C., Tilton, S. C., Menachery, V. D., Gralinski, L. E., Schafer, A., Matzke, M. M.,
802 Webb-Robertson, B.-J. M., Chang, J., Luna, M. L., Long, C. E., Shukla, A. K.,
803 Bankhead, A. R. 3rd, Burkett, S. E., Zornetzer, G., Tseng, C.-T. K., Metz, T. O.,
804 Pickles, R., McWeeney, S., Smith, R. D., … Baric, R. S. (2013). Release of severe
805 acute respiratory syndrome coronavirus nuclear import block enhances host
806 transcription in human lung cells. *Journal of Virology*, *87*(7), 3885–3902.
807 https://doi.org/10.1128/JVI.02520-12

808 Siraj, A. K., Pratheeshkumar, P., Divya, S. P., Parvathareddy, S. K., Bu, R., Masoodi,
809 T., Kong, Y., Thangavel, S., Al-Sanea, N., Ashari, L. H., Abduljabbar, A., Al-
810 Homoud, S., Al-Dayel, F., & Al-Kuraya, K. S. (2019). TGFbeta-induced SMAD4-
811 dependent Apoptosis Proceeded by EMT in CRC. *Molecular Cancer Therapeutics*,
812 *18*(7), 1312–1322. https://doi.org/10.1158/1535-7163.MCT-18-1378

813 Siston, A. M., Rasmussen, S. A., Honein, M. A., Fry, A. M., Seib, K., Callaghan, W. M.,
814 Louie, J., Doyle, T. J., Crockett, M., Lynfield, R., Moore, Z., Wiedeman, C., Anand,
815 M., Tabony, L., Nielsen, C. F., Waller, K., Page, S., Thompson, J. M., Avery, C., …
816 Jamieson, D. J. (2010). Pandemic 2009 influenza A(H1N1) virus illness among
817 pregnant women in the United States. *JAMA*, *303*(15), 1517–1525.
818 https://doi.org/10.1001/jama.2010.479

819 Stark, G. R., Kerr, I. M., Williams, B. R., Silverman, R. H., & Schreiber, R. D. (1998).
820 How cells respond to interferons. *Annual Review of Biochemistry*, *67*, 227–264.
821 https://doi.org/10.1146/annurev.biochem.67.1.227

822 Subramanian, A., Tamayo, P., Mootha, V. K., Mukherjee, S., Ebert, B. L., Gillette, M. A.,
823 Paulovich, A., Pomeroy, S. L., Golub, T. R., Lander, E. S., & Mesirov, J. P. (2005).

824 Gene set enrichment analysis: a knowledge-based approach for interpreting
825 genome-wide expression profiles. *Proceedings of the National Academy of*
826 *Sciences of the United States of America*, *102*(43), 15545–15550.
827 https://doi.org/10.1073/pnas.0506580102

828 Suh, Y., Yoon, C.-H., Kim, R.-K., Lim, E.-J., Oh, Y. S., Hwang, S.-G., An, S., Yoon, G.,
829 Gye, M. C., Yi, J.-M., Kim, M.-J., & Lee, S.-J. (2013). Claudin-1 induces epithelial-
830 mesenchymal transition through activation of the c-Abl-ERK signaling pathway in
831 human liver cells. *Oncogene*, *32*(41), 4873–4882.
832 https://doi.org/10.1038/onc.2012.505

833 Takahashi, K., Halfmann, P., Oyama, M., Kozuka-Hata, H., Noda, T., & Kawaoka, Y.
834 (2013). DNA topoisomerase 1 facilitates the transcription and replication of the
835 Ebola virus genome. *Journal of Virology*, *87*(16), 8862–8869.
836 https://doi.org/10.1128/JVI.03544-12

837 Takeda, K., Kaisho, T., & Akira, S. (2003). Toll-like receptors. *Annual Review of*
838 *Immunology*, *21*, 335–376.
839 https://doi.org/10.1146/annurev.immunol.21.120601.141126

840 Taki, M., Abiko, K., Baba, T., Hamanishi, J., Yamaguchi, K., Murakami, R., Yamanoi, K.,
841 Horikawa, N., Hosoe, Y., Nakamura, E., Sugiyama, A., Mandai, M., Konishi, I., &
842 Matsumura, N. (2018). Snail promotes ovarian cancer progression by recruiting
843 myeloid-derived suppressor cells via CXCR2 ligand upregulation. *Nature*
844 *Communications*, *9*(1), 1685. https://doi.org/10.1038/s41467-018-03966-7

845 Tecalco-Cruz, A. C., Rios-Lopez, D. G., Vazquez-Victorio, G., Rosales-Alvarez, R. E., &
846 Macias-Silva, M. (2018). Transcriptional cofactors Ski and SnoN are major
847 regulators of the TGF-beta/Smad signaling pathway in health and disease. *Signal*
848 *Transduction and Targeted Therapy*, *3*, 15. https://doi.org/10.1038/s41392-018-
849 0015-8

850 Totura, A. L., & Bavari, S. (2019). Broad-spectrum coronavirus antiviral drug discovery.
851 *Expert Opinion on Drug Discovery*, *14*(4), 397–412.
852 https://doi.org/10.1080/17460441.2019.1581171

853 Totura, A. L., Whitmore, A., Agnihothram, S., Schafer, A., Katze, M. G., Heise, M. T., &
854 Baric, R. S. (2015). Toll-Like Receptor 3 Signaling via TRIF Contributes to a
855 Protective Innate Immune Response to Severe Acute Respiratory Syndrome
856 Coronavirus Infection. *MBio*, *6*(3), e00638-15. https://doi.org/10.1128/mBio.00638-
857 15

858 Vukmirovic, M., Herazo-Maya, J. D., Blackmon, J., Skodric-Trifunovic, V., Jovanovic, D.,
859 Pavlovic, S., Stojsic, J., Zeljkovic, V., Yan, X., Homer, R., Stefanovic, B., &
860 Kaminski, N. (2017). Identification and validation of differentially expressed
861 transcripts by RNA-sequencing of formalin-fixed, paraffin-embedded (FFPE) lung
862 tissue from patients with Idiopathic Pulmonary Fibrosis. *BMC Pulmonary Medicine*,
863 *17*(1), 15. https://doi.org/10.1186/s12890-016-0356-4

Wan, L. C. K., Maisonneuve, P., Szilard, R. K., Lambert, J.-P., Ng, T. F., Manczyk, N., Huang, H., Laister, R., Caudy, A. A., Gingras, A.-C., Durocher, D., & Sicheri, F. (2017). Proteomic analysis of the human KEOPS complex identifies C14ORF142 as a core subunit homologous to yeast Gon7. *Nucleic Acids Research*, *45*(2), 805–817. https://doi.org/10.1093/nar/gkw1181

Wang, C.-A., Drasin, D., Pham, C., Jedlicka, P., Zaberezhnyy, V., Guney, M., Li, H., Nemenoff, R., Costello, J. C., Tan, A.-C., & Ford, H. L. (2014). Homeoprotein Six2 promotes breast cancer metastasis via transcriptional and epigenetic control of E-cadherin expression. *Cancer Research*, *74*(24), 7357–7370. https://doi.org/10.1158/0008-5472.CAN-14-0666

Wang, C., Zhang, J., Fok, K. L., Tsang, L. L., Ye, M., Liu, J., Li, F., Zhao, A. Z., Chan, H. C., & Chen, H. (2018). CD147 Induces Epithelial-to-Mesenchymal Transition by Disassembling Cellular Apoptosis Susceptibility Protein/E-Cadherin/beta-Catenin Complex in Human Endometriosis. *The American Journal of Pathology*, *188*(7), 1597–1607. https://doi.org/10.1016/j.ajpath.2018.03.004

Wang, K., & Li, J. (2016). Overexpression of ANXA3 is an independent prognostic indicator in gastric cancer and its depletion suppresses cell proliferation and tumor growth. *Oncotarget*, *7*(52), 86972–86984. https://doi.org/10.18632/oncotarget.13493

Wang, S., Lei, T., Zhang, K., Zhao, W., Fang, L., Lai, B., Han, J., Xiao, L., & Wang, N. (2014). Xenobiotic pregnane X receptor (PXR) regulates innate immunity via activation of NLRP3 inflammasome in vascular endothelial cells. *The Journal of Biological Chemistry*, *289*(43), 30075–30081. https://doi.org/10.1074/jbc.M114.578781

Wang, W., Ye, L., Ye, L., Li, B., Gao, B., Zeng, Y., Kong, L., Fang, X., Zheng, H., Wu, Z., & She, Y. (2007). Up-regulation of IL-6 and TNF-alpha induced by SARS-coronavirus spike protein in murine macrophages via NF-kappaB pathway. *Virus Research*, *128*(1–2), 1–8. https://doi.org/10.1016/j.virusres.2007.02.007

Wei, C.-Y., Zhu, M.-X., Yang, Y.-W., Zhang, P.-F., Yang, X., Peng, R., Gao, C., Lu, J.-C., Wang, L., Deng, X.-Y., Lu, N.-H., Qi, F.-Z., & Gu, J.-Y. (2019). Downregulation of RNF128 activates Wnt/beta-catenin signaling to induce cellular EMT and stemness via CD44 and CTTN ubiquitination in melanoma. *Journal of Hematology & Oncology*, *12*(1), 21. https://doi.org/10.1186/s13045-019-0711-z

Wobbe, C. R., Dean, F. B., Murakami, Y., Borowiec, J. A., Bullock, P., & Hurwitz, J. (1987). In vitro replication of DNA containing either the SV40 or the polyoma origin. *Philosophical Transactions of the Royal Society of London. Series B, Biological Sciences*, *317*(1187), 439–453. https://doi.org/10.1098/rstb.1987.0071

Xia, L., Dai, L., Yu, Q., & Yang, Q. (2017). Persistent Transmissible Gastroenteritis Virus Infection Enhances Enterotoxigenic Escherichia coli K88 Adhesion by Promoting Epithelial-Mesenchymal Transition in Intestinal Epithelial Cells. *Journal of Virology*, *91*(21). https://doi.org/10.1128/JVI.01256-17

905 Xu, C.-B., Liu, X.-S.-B.-J., Li, J.-Q., Zhao, X., Xin, D., & Yu, D. (2019). microRNA-539
906 functions as a tumor suppressor in papillary thyroid carcinoma via the transforming
907 growth factor beta1/Smads signaling pathway by targeting secretory leukocyte
908 protease inhibitor. *Journal of Cellular Biochemistry*, *120*(6), 10830–10846.
909 https://doi.org/10.1002/jcb.28374

910 Yamajuku, D., Shibata, Y., Kitazawa, M., Katakura, T., Urata, H., Kojima, T., Nakata, O.,
911 & Hashimoto, S. (2010). Identification of functional clock-controlled elements
912 involved in differential timing of Per1 and Per2 transcription. *Nucleic Acids*
913 *Research*, *38*(22), 7964–7973. https://doi.org/10.1093/nar/gkq678

914 Yang, J., Deng, X., Deng, L., Gu, H., Fan, W., & Cao, Y. (2004). Telomerase activation
915 by Epstein-Barr virus latent membrane protein 1 is associated with c-Myc
916 expression in human nasopharyngeal epithelial cells. *Journal of Experimental &*
917 *Clinical Cancer Research : CR*, *23*(3), 495–506.

918 Yin, L., Hubbard, A. K., & Giardina, C. (2000). NF-kappa B regulates transcription of the
919 mouse telomerase catalytic subunit. *The Journal of Biological Chemistry*, *275*(47),
920 36671–36675. https://doi.org/10.1074/jbc.M007378200

921 Yoshikawa, T., Hill, T. E., Yoshikawa, N., Popov, V. L., Galindo, C. L., Garner, H. R.,
922 Peters, C. J., & Tseng, C.-T. K. (2010). Dynamic innate immune responses of
923 human bronchial epithelial cells to severe acute respiratory syndrome-associated
924 coronavirus infection. *PloS One*, *5*(1), e8729.
925 https://doi.org/10.1371/journal.pone.0008729

926 Zaborowska, J., Isa, N. F., & Murphy, S. (2016). P-TEFb goes viral. *BioEssays : News*
927 *and Reviews in Molecular, Cellular and Developmental Biology*, *38 Suppl 1*, S75-
928 85. https://doi.org/10.1002/bies.201670912

929 Zhang, L., Wang, X., Lai, C., Zhang, H., & Lai, M. (2019). PMEPA1 induces EMT via a
930 non-canonical TGF-beta signalling in colorectal cancer. *Journal of Cellular and*
931 *Molecular Medicine*, *23*(5), 3603–3615. https://doi.org/10.1111/jcmm.14261

932 Zhao, M., Kong, L., Liu, Y., & Qu, H. (2015). dbEMT: an epithelial-mesenchymal
933 transition associated gene resource. *Scientific Reports*, *5*, 11459.
934 https://doi.org/10.1038/srep11459

935 Zheng, K., Kitazato, K., & Wang, Y. (2014). Viruses exploit the function of epidermal
936 growth factor receptor. *Reviews in Medical Virology*, *24*(4), 274–286.
937 https://doi.org/10.1002/rmv.1796

938 Zhou, F., Geng, J., Xu, S., Meng, Q., Chen, K., Liu, F., Yang, F., Pan, B., & Yu, Y.
939 (2019). FAM83A signaling induces epithelial-mesenchymal transition by the
940 PI3K/AKT/Snail pathway in NSCLC. *Aging*, *11*(16), 6069–6088.
941 https://doi.org/10.18632/aging.102163

942 Zhou, P., Yang, X.-L., Wang, X.-G., Hu, B., Zhang, L., Zhang, W., Si, H.-R., Zhu, Y., Li,
943 B., Huang, C.-L., Chen, H.-D., Chen, J., Luo, Y., Guo, H., Jiang, R.-D., Liu, M.-Q.,

944 Chen, Y., Shen, X.-R., Wang, X., … Shi, Z.-L. (2020). A pneumonia outbreak
945 associated with a new coronavirus of probable bat origin. *Nature*, *579*(7798), 270–
946 273. https://doi.org/10.1038/s41586-020-2012-7

947

948

Figure Titles Legends

Figure 1. Ranking of ISGs in the human ALL CoV infection transcriptomic consensome. See Supplementary information, Section 2, column I.

Figure 2. GeneOverlap analysis of CoV and IAV TC95s and SPP receptor or enzyme TC95s. OR: Odds ratio. All ORs are $p < 0.05$. Numerical data are provided in Supplementary information Section 8.

Figure 3. GeneOverlap analysis of CoV and IAV TC95s and ChIP-Atlas transcription factor CC95s. OR: Odds ratio. All ORs are $p < 0.05$. Numerical data are provided in Supplementary information Section 8.

Figure 4. GeneOverlap analysis of CoV and IAV TC95s and ChIP-Atlas enzyme CC95s. OR: Odds ratio. Numerical data are provided in Supplementary information Section 8. All ORs are $p < 0.05$.

Figure 5. GeneOverlap analysis of CoV and IAV TC95s and ChIP-Atlas co-node CC95s. OR: Odds ratio. Numerical data are provided in Supplementary information Section 8. All ORs are $p < 0.05$.

Figure 6. Antagonism between PGR and IFNR signaling in the regulation of viral response genes in the airway epithelium. PGR loss of function experiments were retrieved from GSE17307 (SPP DOI 10.1621/ xigKzGn1se).

Figure 7. Conservation of polarity of differential expression in CoV, IFNR and TERT perturbation transcriptomic experiments across diverse canonical interferon-inducible viral response genes. Positive/negative regulatory relationship of TERT with a transcriptional target was inferred from the design of the underlying

971 experiments: this was loss of function for experiments in GSE77014 (MST132 inhibitor)
972 and GSE60175 (shRNA), and gain of function in E-MEXP-563 (overexpression). All
973 IFNR experiments were gain of function using characterized physiological ligands for
974 members of the family.

975 **Figure 8. Identification of a SARS2 epithelial to mesenchymal transcriptional**
976 **signature.** Note that the SARS2 genes are all in the 99th percentile and are therefore
977 superimposed in the scatterplot. Indicated are the results of the Paired Two Sample for
978 Means t-Test comparing the Relative Ranks of the genes in the SARS2 consensome
979 with those in the SARS1, MERS and IAV consensomes.

980

Tables

Table 1. Genes in the 99th %ile of the ALL CoV consensome and the 50th percentile of the IAV consensome

		CONSENSOME %ILE	
Symbol	**Name**	All CoV	IAV
GEM	GTP binding protein overexpressed in skeletal muscle	99	43
DHRS1	dehydrogenase/reductase 1	99	43
NIPSNAP3A	nipsnap homolog 3A	99	43
SFSWAP	splicing factor SWAP	99	43
GON7	GON7 subunit of KEOPS complex	99	39
INHBA	inhibin subunit beta A	99	37
PDZK1	PDZ domain containing 1	99	37
PER1	period circadian regulator 1	99	33
PAQR6	progestin and adipoQ receptor family member 6	99	33
IFT20	intraflagellar transport 20	99	33
ZNF628	zinc finger protein 628	99	33
KANSL1	KAT8 regulatory NSL complex subunit 1	99	33
CREB5	cAMP responsive element binding protein 5	99	27
PER2	period circadian regulator 2	99	17
TJAP1	tight junction associated protein 1	99	17

987 **Table 2. Links to SPP Regulation Reports for the top 20 ranked genes in the ALL**

988 **CoV consensome**

Symbol	Name	Link
JUN	Jun proto-oncogene, AP-1 transcription factor subunit	SPP Regulation Report
DUSP1	dual specificity phosphatase 1	SPP Regulation Report
FOS	Fos proto-oncogene, AP-1 transcription factor subunit	SPP Regulation Report
EGR1	early growth response 1	SPP Regulation Report
CXCL2	C-X-C motif chemokine ligand 2	SPP Regulation Report
TNFAIP3	TNF alpha induced protein 3	SPP Regulation Report
IER2	immediate early response 2	SPP Regulation Report
CCNL1	cyclin L1	SPP Regulation Report
PIM3	Pim-3 proto-oncogene, serine/threonine kinase	SPP Regulation Report
CSRNP1	cysteine and serine rich nuclear protein 1	SPP Regulation Report
FOSB	FosB proto-oncogene, AP-1 transcription factor subunit	SPP Regulation Report
ZC3H12A	zinc finger CCCH-type containing 12A	SPP Regulation Report
ZFP36	ZFP36 ring finger protein	SPP Regulation Report
BHLHE40	basic helix-loop-helix family member e40	SPP Regulation Report
RELB	RELB proto-oncogene, NF-kB subunit	SPP Regulation Report
EGR2	early growth response 2	SPP Regulation Report
NFKBIA	NFKB inhibitor alpha	SPP Regulation Report
BCL3	BCL3 transcription coactivator	SPP Regulation Report
YRDC	yrdC N6-threonylcarbamoyltransferase domain containing	SPP Regulation Report
IFIT1	interferon induced protein with tetratricopeptide repeats 1	SPP Regulation Report

989

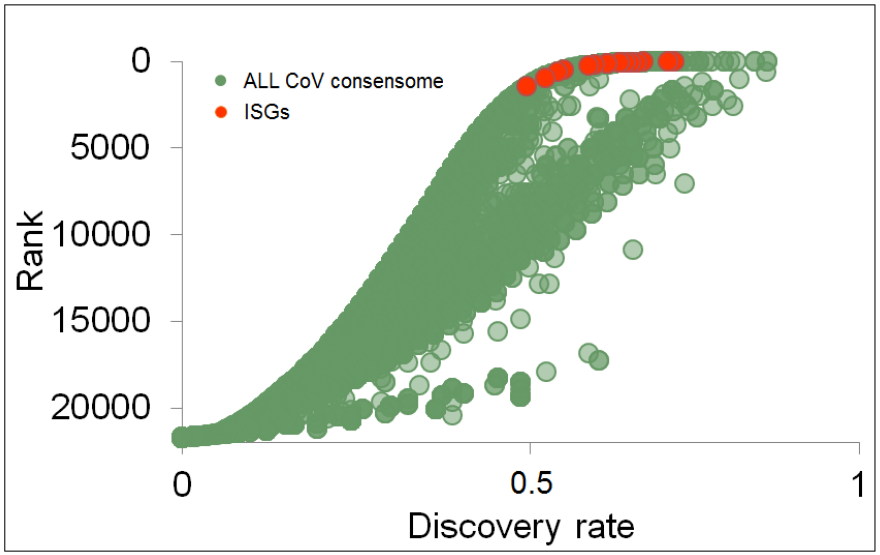

Interferon-stimulated genes (ISG)		ALL CoV CONSENSOME			
Symbol	Name	DR	CPV	Rank	%ile
IFIT1	interferon induced protein with tetratricopeptide repeats 1	0.73	1.5E-78	20	99
IFIT3	interferon induced protein with tetratricopeptide repeats 3	0.72	7.4E-77	25	99
IFI35	interferon induced protein 35	0.72	7.4E-77	28	99
ISG20	interferon stimulated exonuclease gene 20	0.68	2.8E-70	55	99
IFIT2	interferon induced protein with tetratricopeptide repeats 2	0.67	1.1E-68	62	99
ISG15	ISG15 ubiquitin like modifier	0.66	4.2E-67	69	99
IRF9	interferon regulatory factor 9	0.66	4.2E-67	71	99
IFIT5	interferon induced protein with tetratricopeptide repeats 5	0.65	1.5E-65	82	99
MX1	MX dynamin like GTPase 1	0.65	5.4E-64	89	99
IFIH1	interferon induced with helicase C domain 1	0.65	5.4E-64	91	99
IFITM3	interferon induced transmembrane protein 3	0.65	5.4E-64	94	99
IFITM1	interferon induced transmembrane protein 1	0.63	5.9E-61	135	99
IRF7	interferon regulatory factor 7	0.63	5.9E-61	138	99
IFITM2	interferon induced transmembrane protein 2	0.63	5.9E-61	140	99
OAS1	2'-5'-oligoadenylate synthetase 1	0.61	5.6E-58	197	99
IFI16	interferon gamma inducible protein 16	0.60	1.6E-56	259	98
DDX58	DExD/H-box helicase 58	0.56	7.8E-51	520	97
IFI27	interferon alpha inducible protein 27	0.55	1.9E-49	624	96
IFI30	IFI30 lysosomal thiol reductase	0.54	9.8E-47	954	95
IFI6	interferon alpha inducible protein 6	0.51	8.9E-43	1472	92

Figure 1

Figure 2

			CORONAVIRUS				
Category	**Class**	**Family**	**ALL**	**SARS1**	**SARS2**	**MERS**	**IAV**
Receptors	Catalytic	Collagen receptors					
		Epidermal growth factor receptors					
		Fibroblast growth factor receptors					
		Insulin receptors					
		Interferon receptors					
		Toll-like receptors					
		Transforming growth factor β receptors					
		Tumor necrosis factor receptors					
	G protein-coupled	Frizzled receptors					
	Nuclear	Androgen receptor					
		Estrogen receptors					
		Estrogen related receptors					
		Glucocorticoid receptor					
		Peroxisome proliferator-activated receptors					
		Progesterone receptor					
		Retinoic acid receptors					
		Retinoid X receptors					
		Vitamin D receptors					
		Xenobiotic Receptors					
	Others	NOTCH receptors					
Enzymes	Kinases	ABL family kinases					
		Cyclin-dependent kinases					
		SRC kinases					
	Telomerases	TERT					
	Topoisomerases	Topoisomerases					

Odds ratio	
	>8
	8
	7
	6
	5
	4
	3
	2
	1

			CORONAVIRUS				
Class	Family	Node	ALL	SARS1	SARS2	MERS	IAV
ARID domain	ARID1 family	ARID1A					
	ARID2 family	ARID2					
	ARID3 family	ARID3A					
BHLH	Ahr-like family	AHR					
		EPAS1					
		HIF1A					
	AP-2 family	TFAP2A					
		TFAP2C					
	AP-4 family	TFAP4					
	Arnt-like factors	ARNT					
		ARNTL					
	E2A-related factors	TCF12					
		TCF3					
		TCF4					
	Hairy-related	BHLHE40					
		HEY1					
	Mad-like factors	MXI1					
	MESP	TCF21					
	Mondo-like factors	MLXIP					
	Myc / Max factors	MAX					
		MYC					
		MYCN					
	Myogenic transcription factors	MYF5					
		MYOD1					
	Neurogenin-Atonal like	NEUROD1					
	SREBP factors	SREBF1					
		SREBF2					
	TFE3-like factors	MITF					
		TFEB					
	Twist-like factors	HAND2					
		USF1					
BZIP	ATF-2-like factors	ATF2					
	ATF-3-like factors	ATF3					
		JDP2					
	ATF-4-related factors	ATF4					
	B-ATF-related factors	BATF					
	C/EBP family	CEBPA					
		CEBPB					
		CEBPD					
		DDIT3					
	CREB-like factors	CREB1					
	Fos factors	FOS					
		FOSL1					
		FOSL2					
	Jun factors	JUN					
		JUNB					
		JUND					
	Large Maf factors	MAF					
	NF-E2-like factors	BACH2					
		NFE2L2					

			CORONAVIRUS				
Class	Family	Node	ALL	SARS1	SARS2	MERS	IAV
	Small Maf factors	MAFG					
		MAFK					
C2H2 Zn finger	B-cell lymphoma 13 (BCL13)	BCL11B					
	B-cell lymphoma 2 (BCL12)	BCL11A					
	BCL6 factors	BCL6					
	CTCF-like	CTCF					
	Early growth response (EGR)	EGR1					
	GFI1 factors	GFI1					
		GLI2					
	Hypermethylated in Cancer	HIC1					
	Ikaros family	IKZF1					
	Kruppel-like	KLF1					
		KLF11					
		KLF4					
		KLF5					
	Kruppel-like	KLF6					
	MAZ-like	MAZ					
	REST	REST					
	Snail-like	SNAI2					
	Sp1-like	SP1					
		SP2					
		SP4					
	ZBTB17	ZBTB17					
	ZBTB7	ZBTB7A					
	ZFX/ZFY factors	ZFX					
	ZNF24-like factors	ZKSCAN1					
	ZNF263	ZNF263					
	ZNF362-like	ZNF384					
	ZNF366-like factors	ZNF366					
	ZNF639-like	ZNF711					
	ZNF76-like	ZNF143					
	ZNF83	ZNF83					
	ZNF92	ZNF92					
	ZNF99-like	ZBTB48					
CXXC zinc finger	CpG-binding proteins	CXXC1					
Fork head / winged helix	E2F family	E2F6					
	FOXA family	FOXA1					
		FOXA2					
	FOXF family	FOXF1					
	FOXK family	FOXK1					
	FOXM family	FOXM1					
	FOXO family	FOXO1					
	FOXP family	FOXP1					
	FOXP family	FOXP2					
	Regulatory factor X (RFX)	RFX5					
Grainyhead domain factors	CP2-related	TFCP2					
Heat shock factors	HSF family	HSF1					
Heteromeric CCAAT	Heteromeric CCAAT-binding	NFYA					
		NFYB					
		NFYC					

Figure 3

Class	Family	Node	CORONAVIRUS ALL	SARS1	SARS2	MERS	IAV
HMG domain	Group B	SOX2					
		SOX3					
	Group E	SOX9					
	TCF-7-related	TCF7L2					
	UBF-related	UBTF					
	WHSC1-related	SSRP1					
Homeo domain	Caudal type homeobox (CDX)	CDX2					
	HNF1-like factors	HNF1B					
	HOX4	HOXA4					
	HOX5 family	HOXC5					
	HOX6-7	HOXA6					
	NK-2.1	NKX2-1					
	Oct-1/2-like (POU2)	POU2F2					
	Orthodenticle homeobox	OTX2					
	PBX	PBX1					
		PBX3					
		PBX4					
	SIX1-like factors	SIX2					
	TLX	TLX1					
	ZHX family	ZHX2					
	Zn finger E-box binding	ZEB1					
MADS box	Myocyte enhancer factor 2	MEF2A					
		MEF2B					
		MEF2C					
	Responders to external signals	SRF					
Nuclear receptors	Androgen receptor	AR					
	COUP-TF-like receptors	NR2F2					
	Estrogen receptors	ESR1					
	Estrogen-related receptors	ESRRA					
	Glucocorticoid receptor	NR3C1					
	HNF4 receptors	HNF4A					
		HNF4G					
	Liver X receptors	NR1H2					
		NR1H3					
	NGFBI-like (NR4A) receptors	NR4A1					
	PPARs	PPARG					
	Progesterone receptor	PGR					
	Retinoid X receptors	RXRA					
	Vitamin D receptor	VDR					
Other C4 zinc finger	Single GATA-type zinc-finger	MTA3					
		TRPS1					
	Two zinc-finger GATA factors	GATA1					
		GATA2					
		GATA3					
		GATA4					
		GATA6					
Other regulators	Canonical HMG	HMGB1					
		HMGB2					
	GTFs	GTF2B					

Class	Family	Node	CORONAVIRUS ALL	SARS1	SARS2	MERS	IAV
	GTFs	GTF2F1					
		GTF3C5					
Others	bromodomain PHD finger	BPTF					
Others	Notch receptors	NOTCH1					
p53 domain	p53-related factors	TP53					
p53 domain		TP63					
Paired box	PAX-2-like factors	PAX5					
Rel Homology Region	Early B-Cell Factor-related	EBF1					
		EBF3					
	IkappaB-related factors	BCL3					
	M	RBPJ					
	NFAT-related factors	NFATC1					
	NF-kappaB p50 subunit-like	NFKB1					
		NFKB2					
		REL					
		RELA					
		RELB					
Runt domain	Core-binding factor subunits	CBFB					
		RUNX1					
		RUNX1T1					
		RUNX2					
		RUNX3					
SMAD/NF1 DBD	Co-activating (Co) Smads	SMAD4					
	Regulatory (R) Smads	SMAD2					
		SMAD3					
STAT domain	STAT factors	STAT1					
		STAT2					
		STAT3					
		STAT4					
		STAT5B					
TATA-binding proteins	TBP-related factors	TBP					
TEA domain	TEF-1-related factors	TEAD1					
		TEAD4					
Tryptophan cluster	EHF-like	ELF3					
	Elf-1-like	ELF1					
	Elk-like	ELK1					
		ELK4					
		ETV1					
		ETV4					
		ETV5					
	Ets-like	ERG					
		FLI1					
		GABPA					
	Interferon-regulatory	IRF1					
		IRF2					
		IRF4					
		IRF8					
	Myb-like	MYB					
		MYBL2					
	Spi-like	SPI1					

Figure 3 (contd)

			CORONAVIRUS				
Class	**Family**	**Node**	**ALL**	**SARS1**	**SARS2**	**MERS**	**IAV**
Acetyltransferases	CBP/p300	CREBBP					
		EP300					
	Lysine acetyltransferases (KAT)	KAT5					
		KAT7					
	Nuclear receptor coactivator (NCOA)	NCOA1					
Deacetylases	Histone deacetylases (HDAC)	HDAC1					
		HDAC2					
Demethylases	Histone-H3-lysine-36 demethylases (KDM)	JMJD1C					
		KDM1A					
		KDM2B					
		KDM4C					
		KDM5A					
		KDM5B					
		KDM5D					
		KDM6A					
		KDM6B					
	jumonji domain containing	JMJD6					
Dioxygenases	Ten-eleven translocation (TET)	TET2					
E3 ubiquitin ligases	Breast cancer associated (BRCA)	BRCA1					
	Cullins (CUL)	CUL4A					
	Protein inhibitor of activated STAT (PIAS)	PIAS1					
	Tripartite motif-containing (TRIM)	TRIM24					
		TRIM25					
		TRIM28					
Helicases	Chromodomain-helicases-DNA binding (CHD)	CHD1					
	ERCC excision repair (ERCC)	ERCC2					
Hydrolases	Recombination activating	RAG1					
		RAG2					
Kinases	Cyclin-dependent kinases (CDK)	CDK6					
		CDK7					
		CDK8					
		CDK9					
	Mammalian target of rapamycin (MTOR)	MTOR					
	Mitogen-activated protein kinases (MAPK)	MAPK14					
	protein kinase, DNA-activated, cat...peptide	PRKDC					
Methyltransferases	DNA (cytosine-5-)-methyltransferases (DNMT)	DNMT3A					
	Histone-lysine N-methyltransferases (KMT)	KMT2A					
		KMT2B					
		KMT2C					
	Protein arginine methyltransferases (PRMT)	PRMT1					
	SET domain-containing (SETD)	SETD1A					
Regulatory factors	Cyclin-dependent kinase inhibitors (CDKN)	CDKN1B					
	Cyclins (CCN)	CCND2					
		CCNT2					
	Protein phosphatase 1 regulatory subunits	APC					
		NONO					
		SFPQ					
Topoisomerases	DNA topoisomerases (TOP)	TOP1					

log10 OR
>1
1
0.9
0.8
0.7
0.6
0.5
0.4
0.3
0.2
0.1

Figure 4

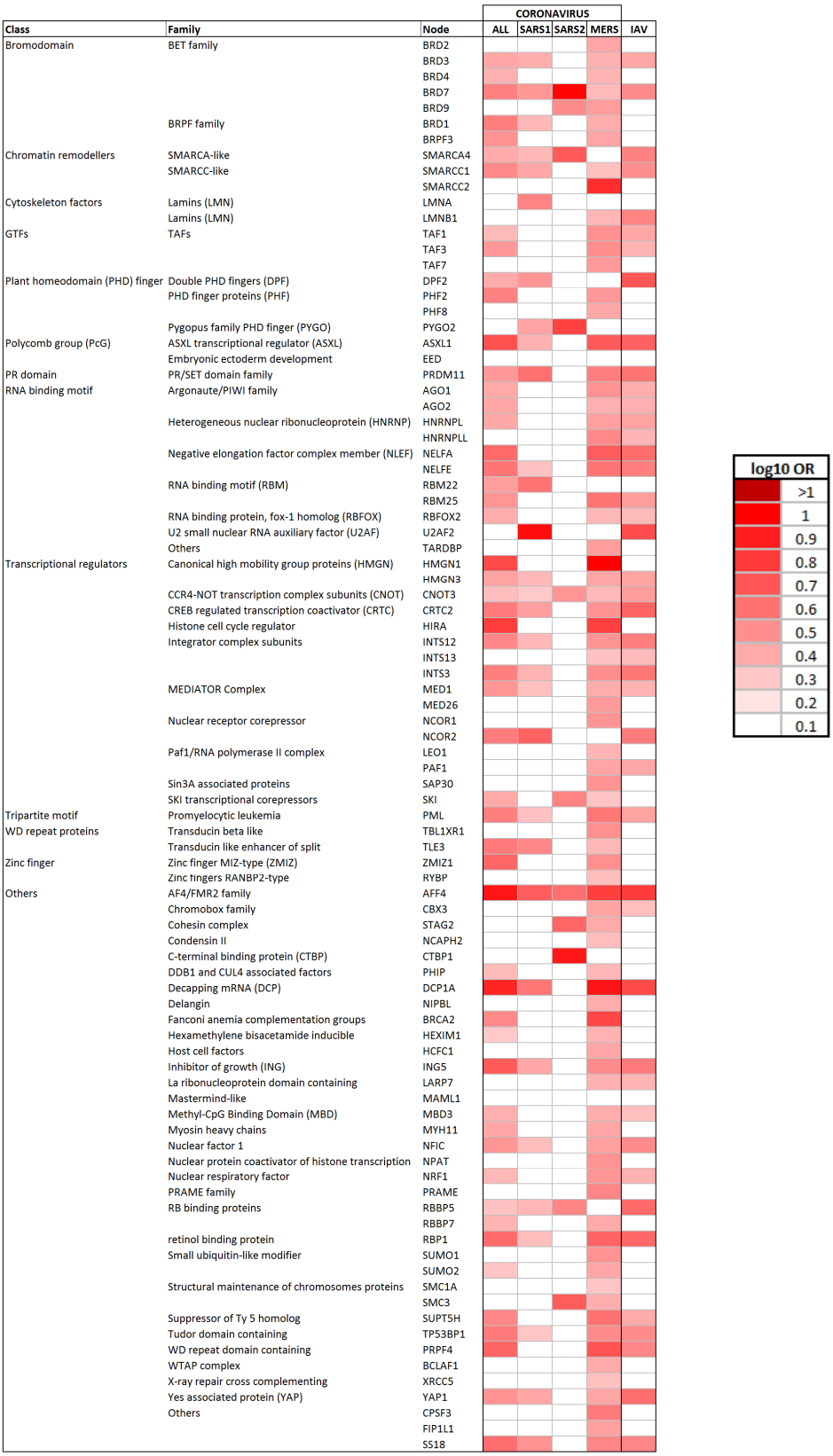

Figure 5

Figure 6

			log10 FC PGR loss of function	
Symbol	**Name**	**log10 FC SARS2**	**RU/DEX vs V**	**RU vs V (DEX)**
CXCL2	C-X-C motif chemokine ligand 2	0.33	0.57	
IL1B	interleukin 1 beta	0.30	0.30	0.29
TNFAIP3	TNF alpha induced protein 3	0.34	0.27	
NFKBIA	NFKB inhibitor alpha	0.19	0.24	
ISG15	ISG15 ubiquitin like modifier	0.88	0.23	0.27
STAT1	signal transducer and activator of transcription 1	0.29	0.21	0.14
ISG20	interferon stimulated exonuclease gene 20	0.14	0.20	0.22
IFI35	interferon induced protein 35	0.32	0.19	0.19
IFITM2	interferon induced transmembrane protein 2	0.14	0.18	0.23
IFIT3	interferon induced protein with tetratricopeptide repeats	0.45	0.16	0.26
OAS1	2'-5'-oligoadenylate synthetase 1	0.49	0.16	0.28
IFITM3	interferon induced transmembrane protein 3	0.24	0.16	0.20
CXXC5	CXXC finger protein 5	-0.14	0.14	0.29
IER3	immediate early response 3	0.20		0.53
MYD88	MYD88 innate immune signal transduction adaptor	0.07		0.19
CXCL1	C-X-C motif chemokine ligand 1	0.32		0.18

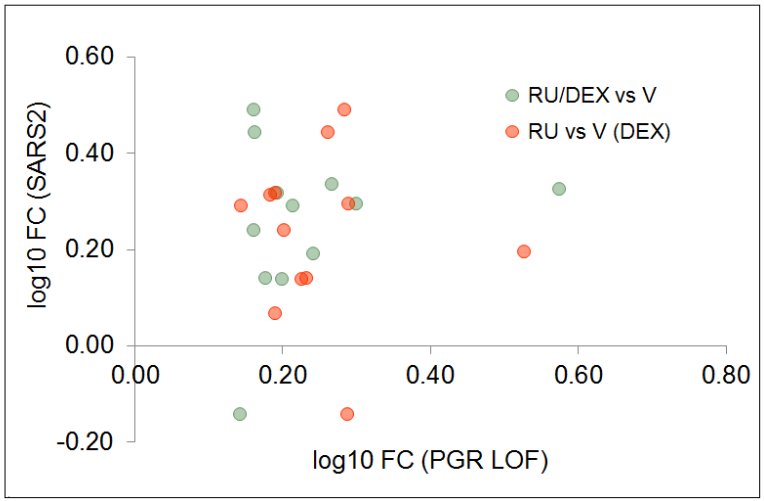

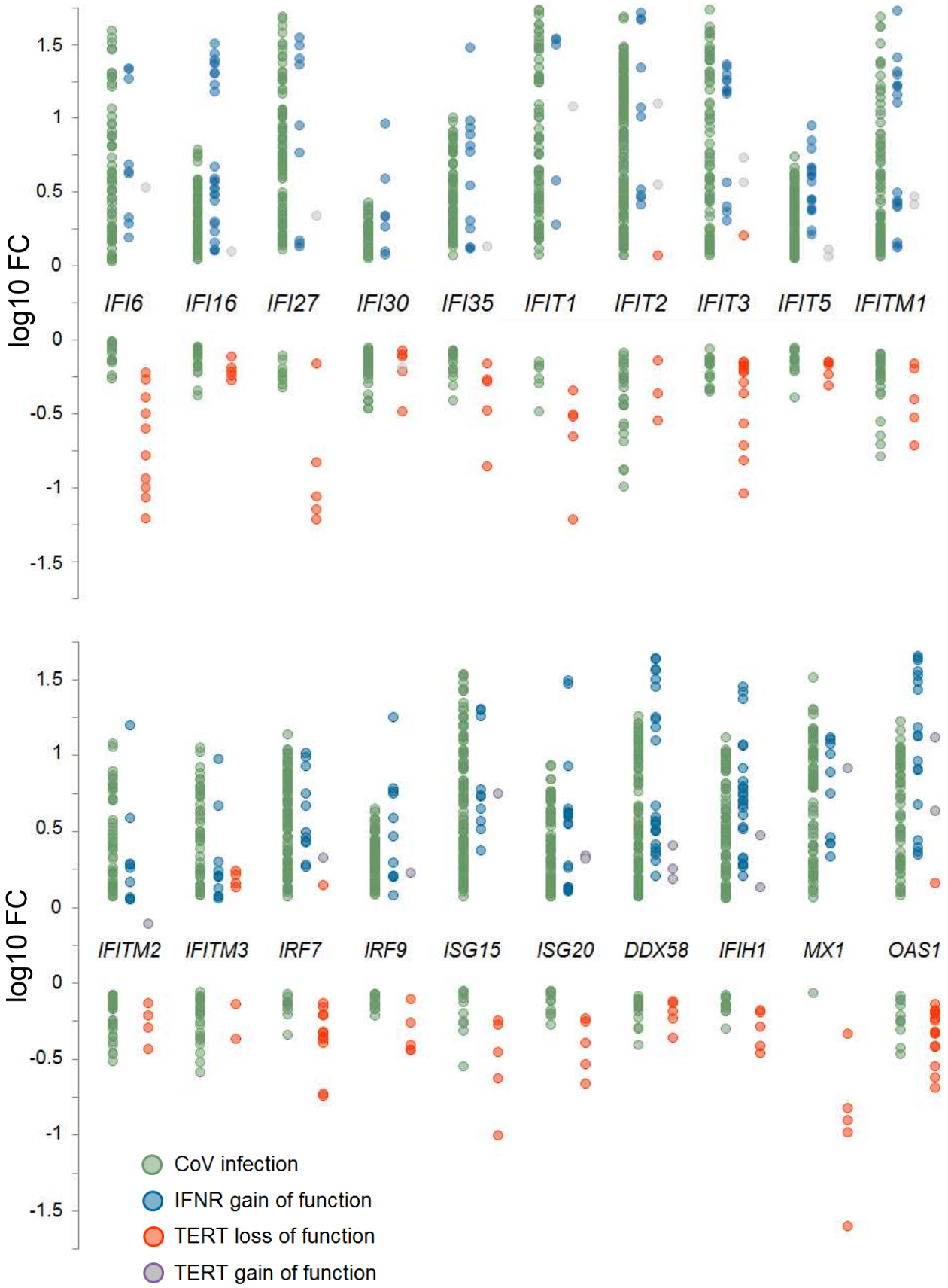

Figure 7

Figure 8

EPITHELIAL TO MESENCHYMAL TRANSITION (EMT) GENES		CONSENSOME %ILE				
Symbol	**Name**	**SARS2**	**SARS1**	**MERS**	**IAV**	**EMT REFERENCE**
ADAR	adenosine deaminase RNA specific	99	96	43	98	Liu et al., 2019
ANXA3	annexin A3	99	80	86	43	Wang & Li, 2016
BIRC3	baculoviral IAP repeat containing 3	99	98	96	94	Mendoza et al., 2017
CLDN1	claudin 1	99	47	83	97	Suh et al., 2013
CXCL2	C-X-C motif chemokine ligand 2	99	99	99	99	Taki et al., 2018
DHDDS	dehydrodolichyl diphosphate synthase subunit	99	23	49	43	Li et al., 2020
FAM83A	family with sequence similarity 83 member A	99	31	3	47	Zhou et al., 2019
IRF9	interferon regulatory factor 9	99	99	91	99	Doherty et al., 2017
KCNMA1	potassium calcium-activated channel subfamily M alpha	99	10	2	10	Kuo et al., 2015
PDE4B	phosphodiesterase 4B	99	61	99	82	Kolosionek et al., 2009
RNF128	ring finger protein 128	99	84	60	86	Wei et al., 2019
RRAGD	Ras related GTP binding D	99	76	79	94	Jordan et al., 2013
SOD2	superoxide dismutase 2	99	84	91	97	Chang et al., 2016